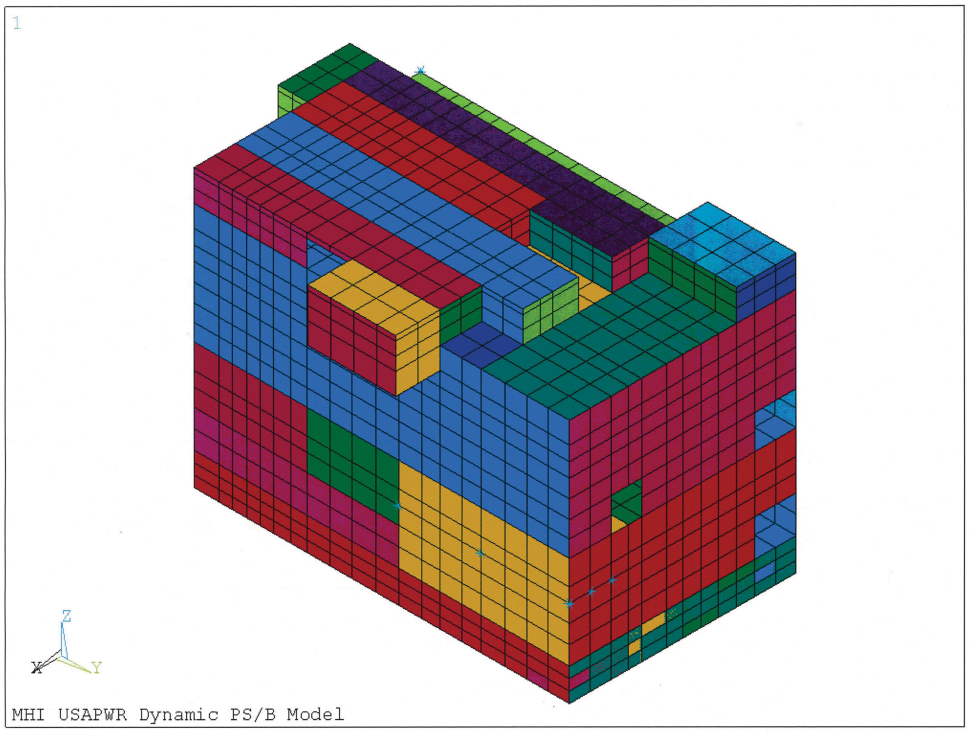

Figure 5.4.1-1 Overview of PS/B Dynamic FE Model

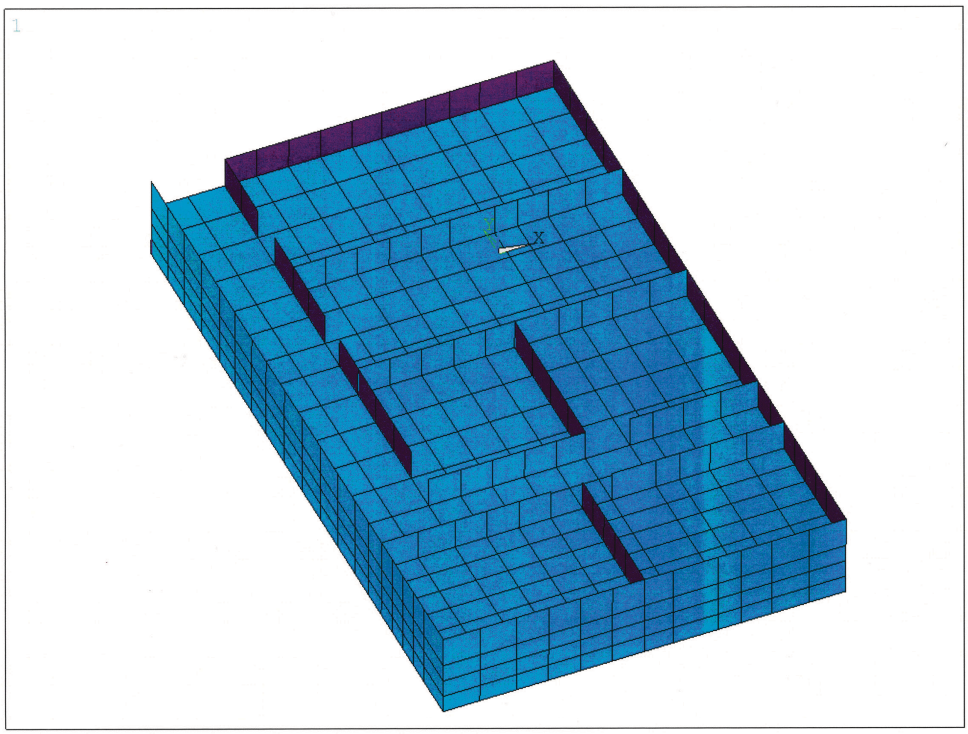

Figure 5.4.1-2 PS/B Dynamic FE Model (EL. -26'-4")

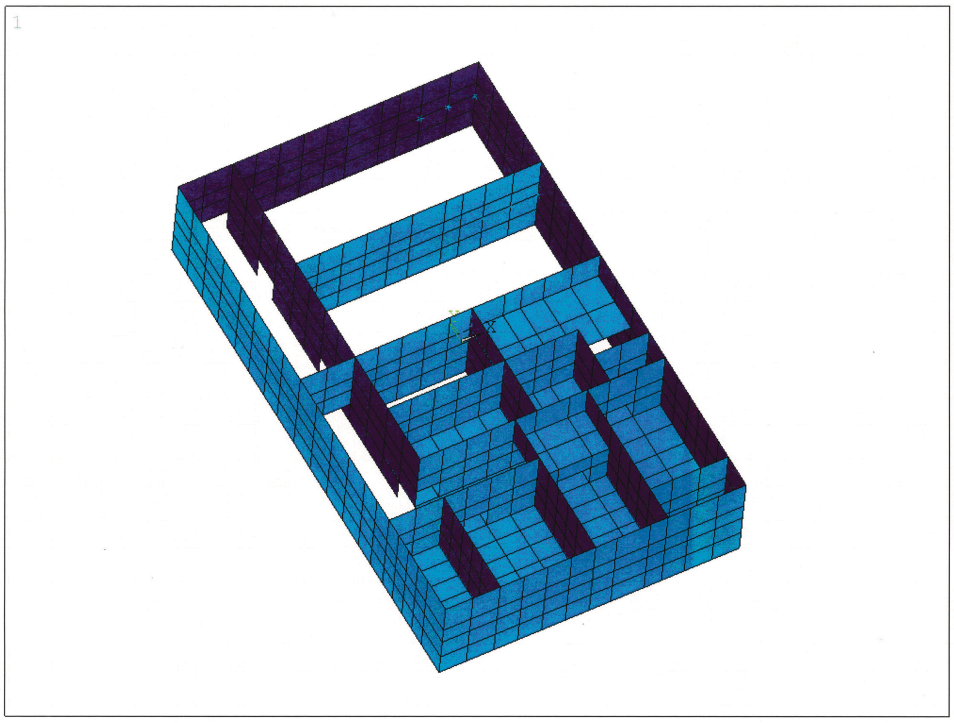

Figure 5.4.1-3 PS/B Dynamic FE Model (EL. -14'-2")

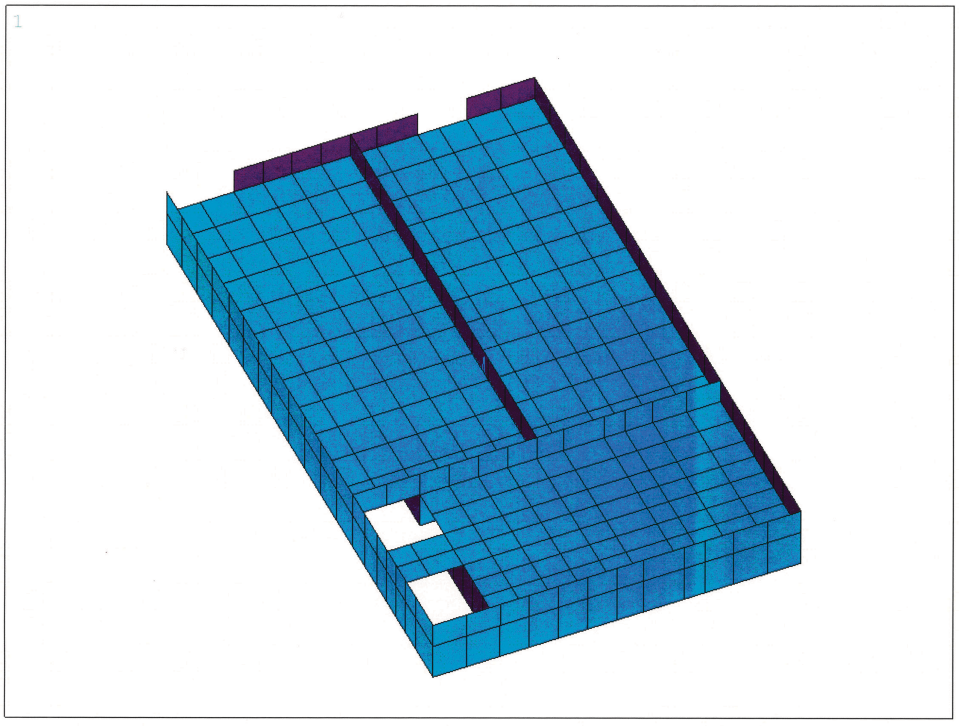

Figure 5.4.1-4 PS/B Dynamic FE Model (EL. -3'-7")

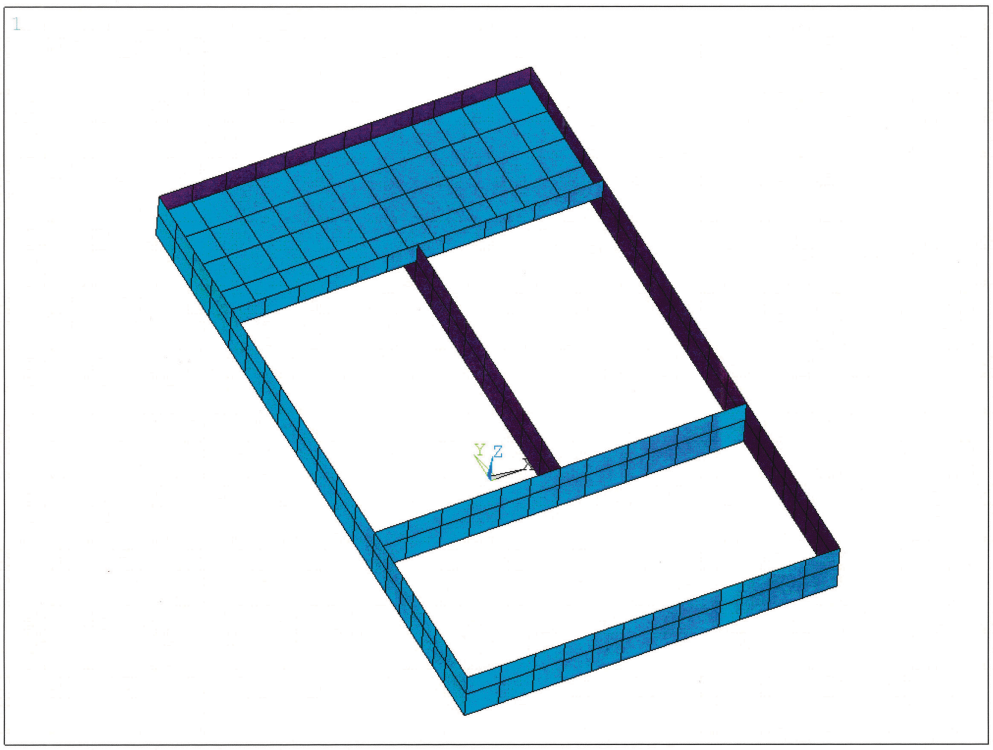

Figure 5.4.1-5 PS/B Dynamic FE Model (EL. 24'-2")

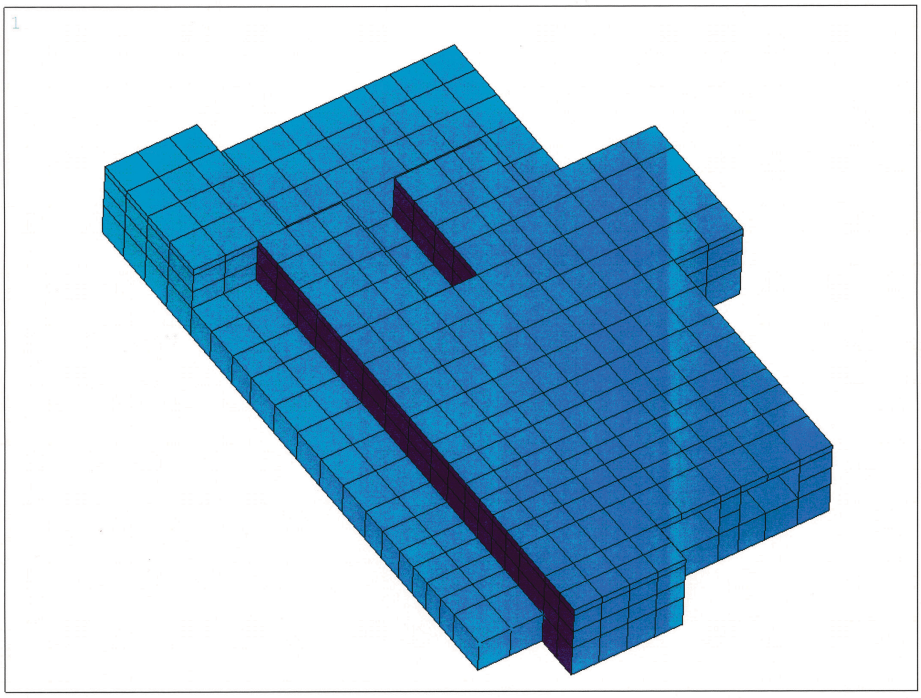

Figure 5.4.1-6 PS/B Dynamic FE Model (Roof – EL. 39'-6" and EL. 49'-0")

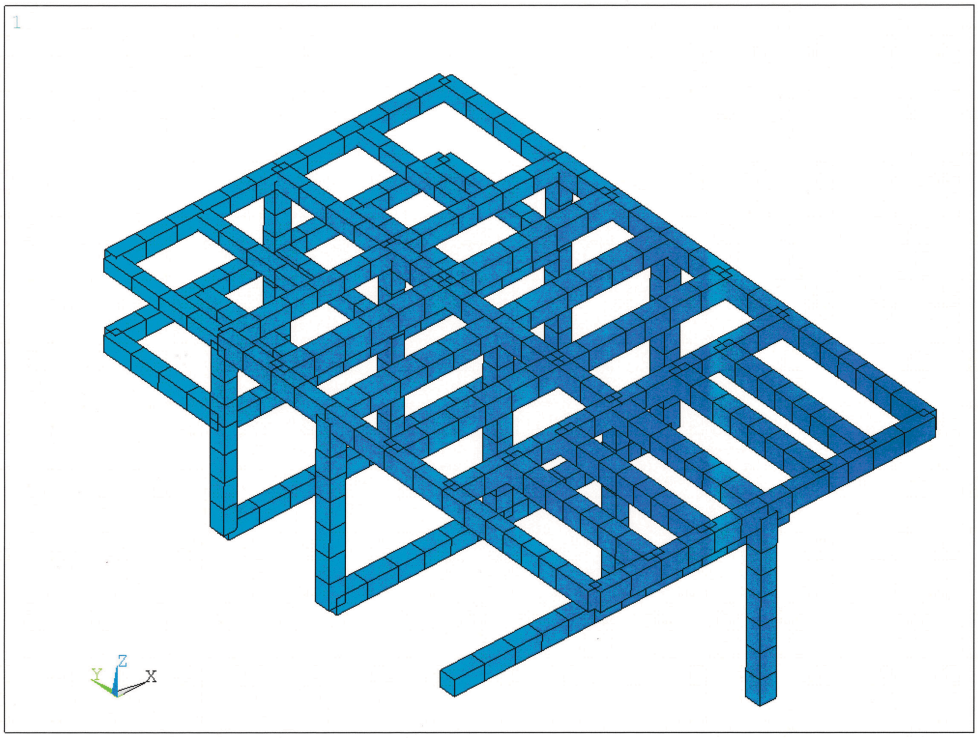

Figure 5.4.1-7 PS/B Dynamic FE Model (Beams and Columns)

5.4.6 Attributes Assigned to the PS/B Dynamic FE Model

The material, sectional properties and dynamic mass attributed to the Dynamic FE model are calculated as per the methodology described in Section 4.4 and its subsections. The attributes of the model include:

- Adjusted material and sectional properties for PS/B walls with and without openings to include applicable additional dynamic masses.
- Adjusted material and sectional properties for PS/B slabs to include applicable additional dynamic masses.
- Material and sectional properties for PS/B beams and columns.

5.4.7 Validation of the PS/B Dynamic FE Model

Validation of the PS/B Dynamic FE Model is carried out in accordance with the methodology described in Section 4.4.3. A summary of these results is presented hereafter.

It is noted that the Detailed PS/B Model utilizes uncracked concrete material properties. Therefore, for comparison and validation purposes, uncracked concrete material properties are also assigned to the Dynamic PS/B Model.

Partial solutions are performed using ANSYS to calculate masses of each floor. The mass of each floor section is taken as the mass of the floor plus that of the walls between the current floor and the floor at the immediate lower elevation. Results in Table 5.4.3-1 indicate that the total mass of the two models are comparable with a difference of 3.74%. The mass differences for each floor section are also acceptable, ranging from 0.44% to 5.92%.

Table 5.4.3-1 PS/B Floor Mass Comparison

Floor	Detailed Model			Dynamic Model			Difference
	Bottom Elev. (ft)	Top Elev. (ft)	Weight (kips)	Bottom Elev.	Top Elev.	Weight (kips)	
B1F Elev. -26'-4"	-36.25	-26.33	12,515	-36.25	-26.33	13,303	5.92%
B1MF Elev. -14'-2"	-26.33	-5.67	6,996	-26.33	-5.33	7,323	4.46%
1F Elev. 3'-7"	-5.67	12.68	9,014	-5.33	12.58	9,153	1.51%
Elev. 24'-2"	12.68	33.21	4,253	12.58	32.29	4,234	-0.44%
Roof Elev. 39'-6"	33.21	38.88	3,976	32.29	38.88	4358	8.78%
Roof Elev. 49'-0"	38.88	48.38	3,144	38.88	48.38	3489	9.89%
Total	--	--	39,898	--	--	41,830	4.62%

5.4.7.1 1g Static Analysis

1g static analysis in the horizontal (X and Y) directions with full constraints at the bottom of the common basemat are performed on both the Detailed and Dynamic FE models of the PS/B.

Displacement results from the 1g static analyses are used to compare the structure stiffness of the two models in the horizontal directions. Lateral displacements in the two horizontal directions (X and Y) along the height of the four corners of both models are plotted in Figures 5.4.3-1 though 5.4.3-8. They all demonstrate that the Dynamic Model lateral stiffness is comparable to that of the Detailed Model (structure behavior follows the same trend for both models) in both directions (X and Y). Table 5.4.3-2 indicates that the maximum roof level lateral displacement difference between the two models varies from 1.22% to 7.94% in the NS (X) direction and from 0.11% to 1.35% in the EW (Y) direction.

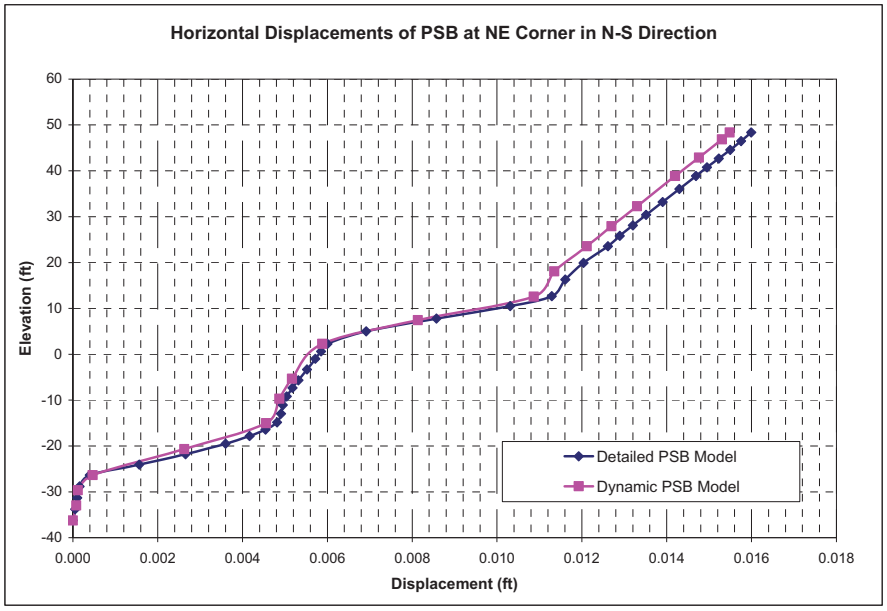

Figure 5.4.3-1 PS/B 1g Static Analysis Results – NS Direction (X) at Northeast Corner

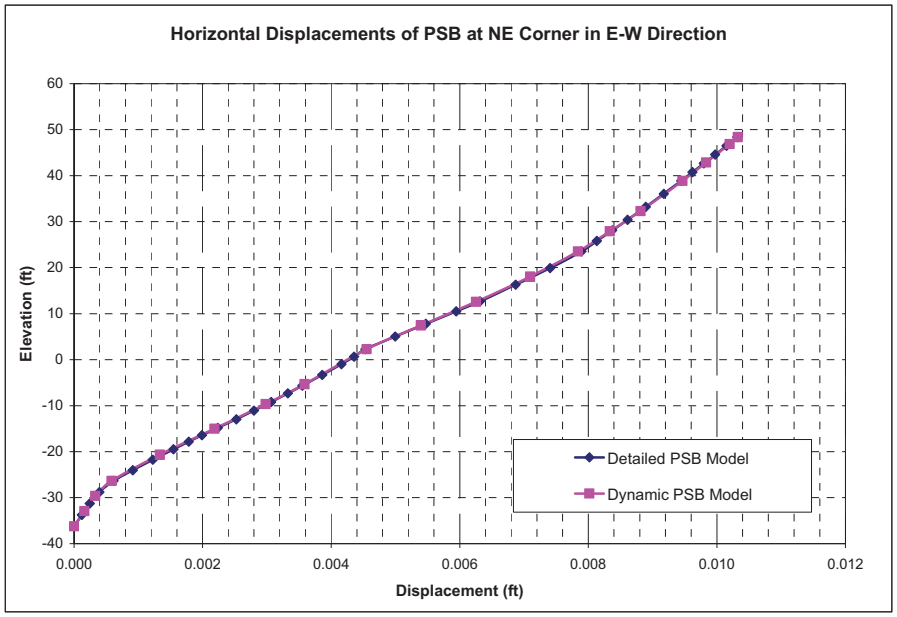

Figure 5.4.3-2 PS/B 1g Static Analysis Results – EW Direction (Y) at Northeast Corner

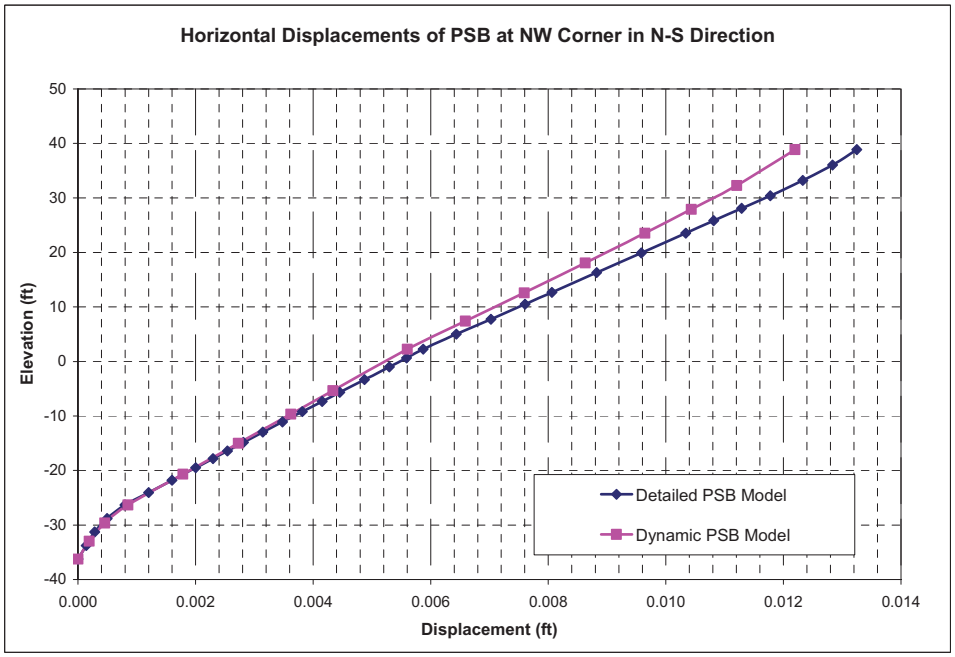

Figure 5.4.3-3 PS/B 1g Static Analysis Results – NS Direction (X) at Northwest Corner

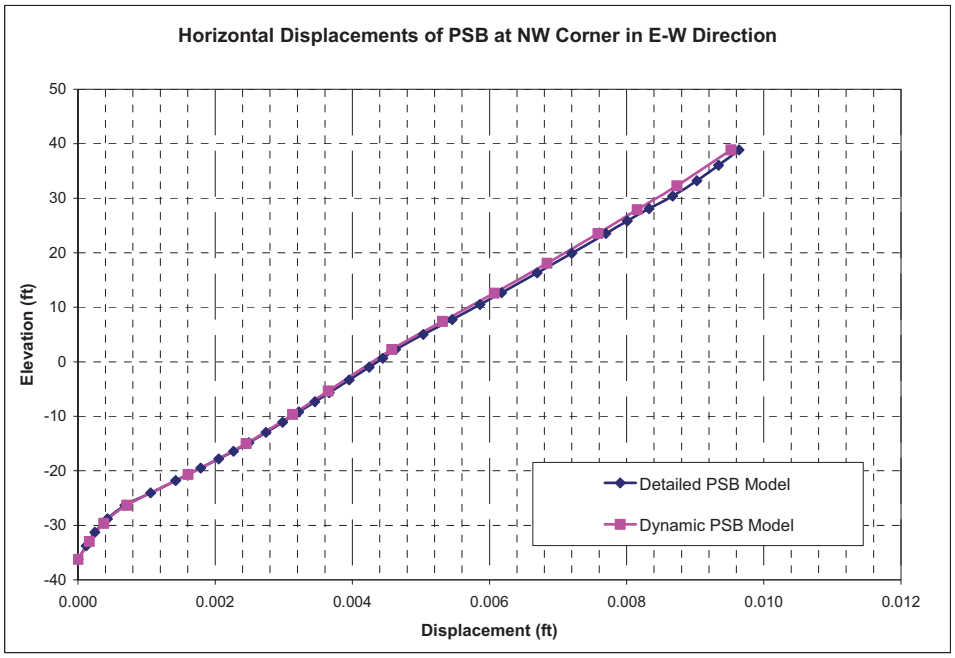

Figure 5.4.3-4 PS/B 1g Static Analysis Results – EW Direction (Y) at Northwest Corner

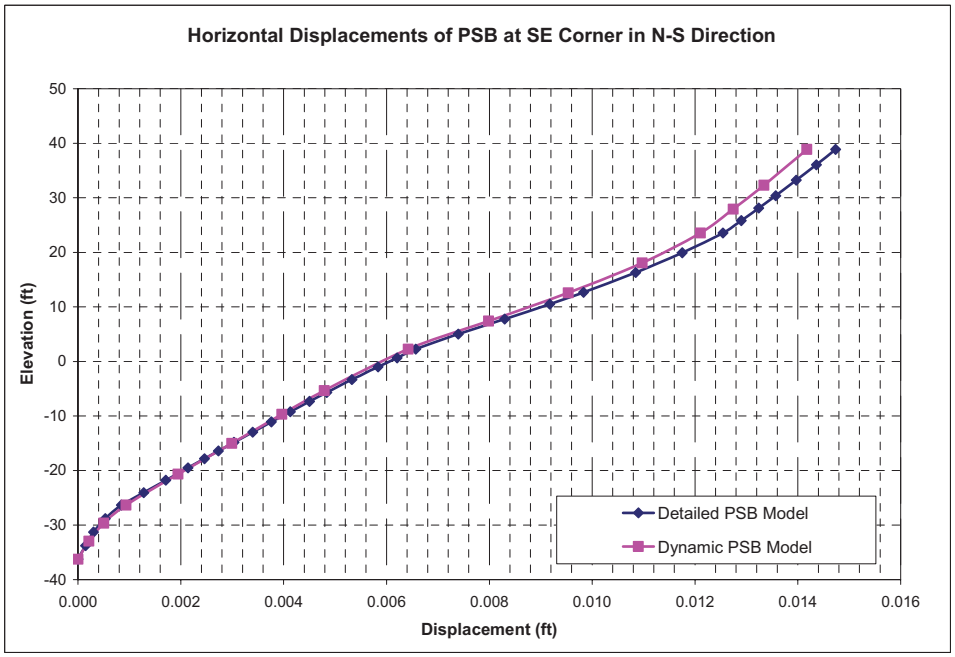

Figure 5.4.3-5 PS/B 1g Static Analysis Results – NS Direction (X) at Southeast Corner

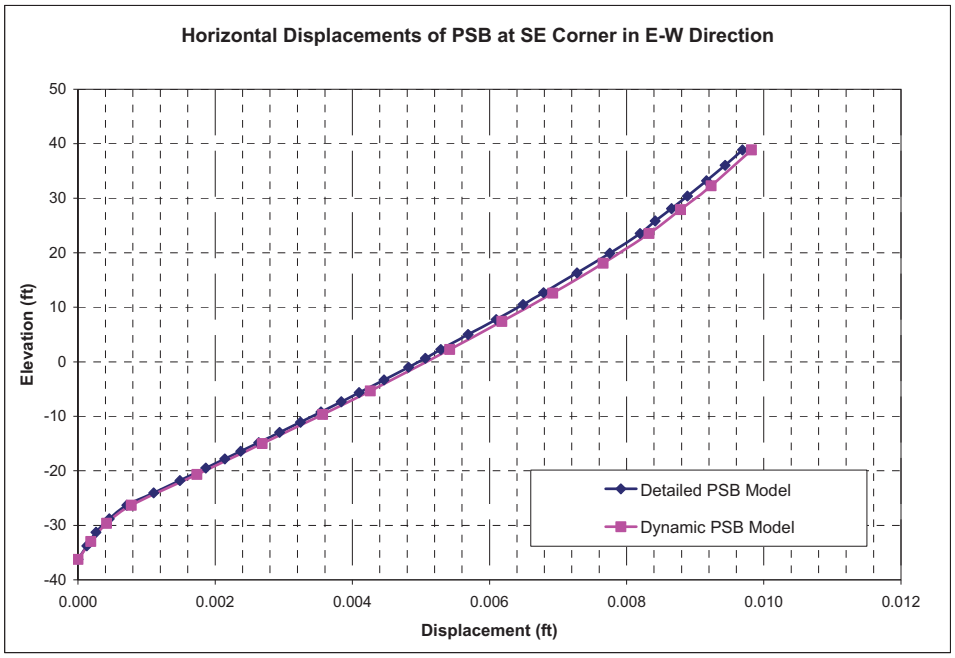

Figure 5.4.3-6 PS/B 1g Static Analysis Results – EW Direction (Y) at Southeast Corner

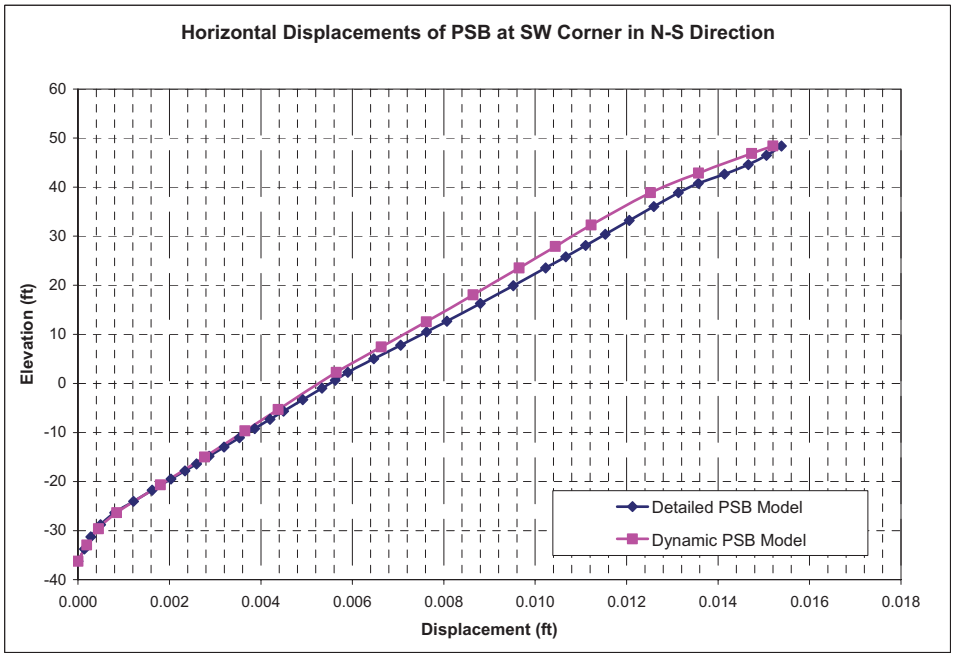

Figure 5.4.3-7 PS/B 1g Static Analysis Results – NS Direction (X) at Southwest Corner

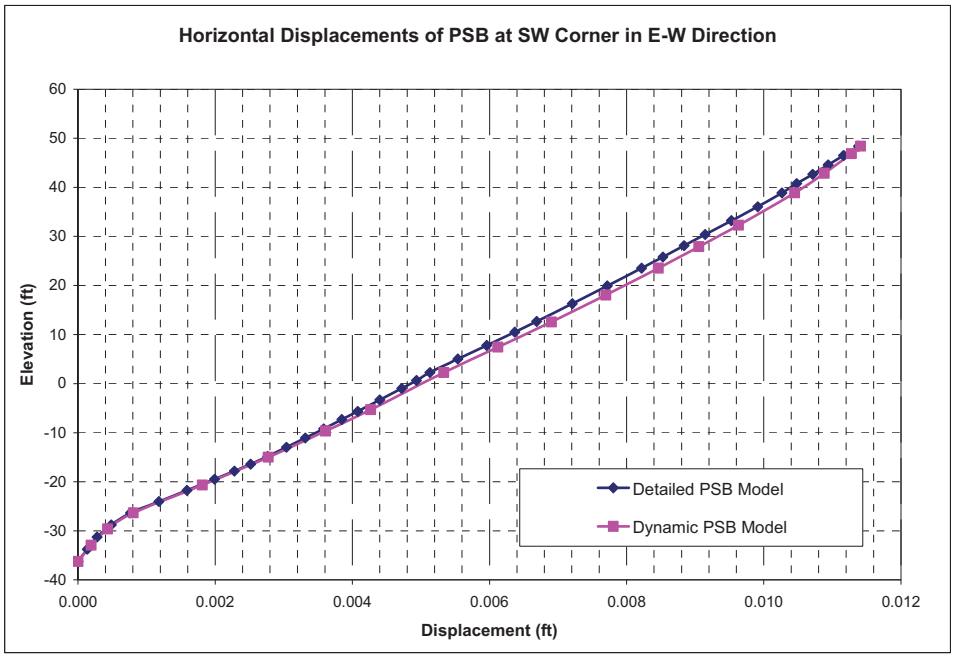

Figure 5.4.3-8 PS/B 1g Static Analysis Results – EW Direction (Y) at Southwest Corner

Table 5.4.3-2 PS/B Roof Lateral Displacement Comparison

Locations	NS Direction			EW Direction		
	Displacement (in)		Difference	Displacement (in)		Difference
	Detailed Model	Dynamic Model		Detailed Model	Dynamic Model	
Northeast	0.0160	0.0155	3.18%	0.0103	0.0103	0.11%
Northwest	0.0132	0.0122	7.94%	0.0096	0.0095	-1.23%
Southeast	0.0147	0.0142	3.79%	0.0097	0.0098	1.35%
Southwest	0.0154	0.0152	1.22%	0.0114	0.0114	-0.27%

5.4.7.2 Modal Analysis

A modal analysis using ANSYS is performed on both the Detailed and the Dynamic FE Models of the PS/B. Plots of Cumulative Mass versus Frequency are shown in Figure 5.4.3-9 through Figure 5.4.3-11. The results of the modal analysis indicate that the Dynamic FE model captures the dynamic properties of the Detailed FE model adequately.

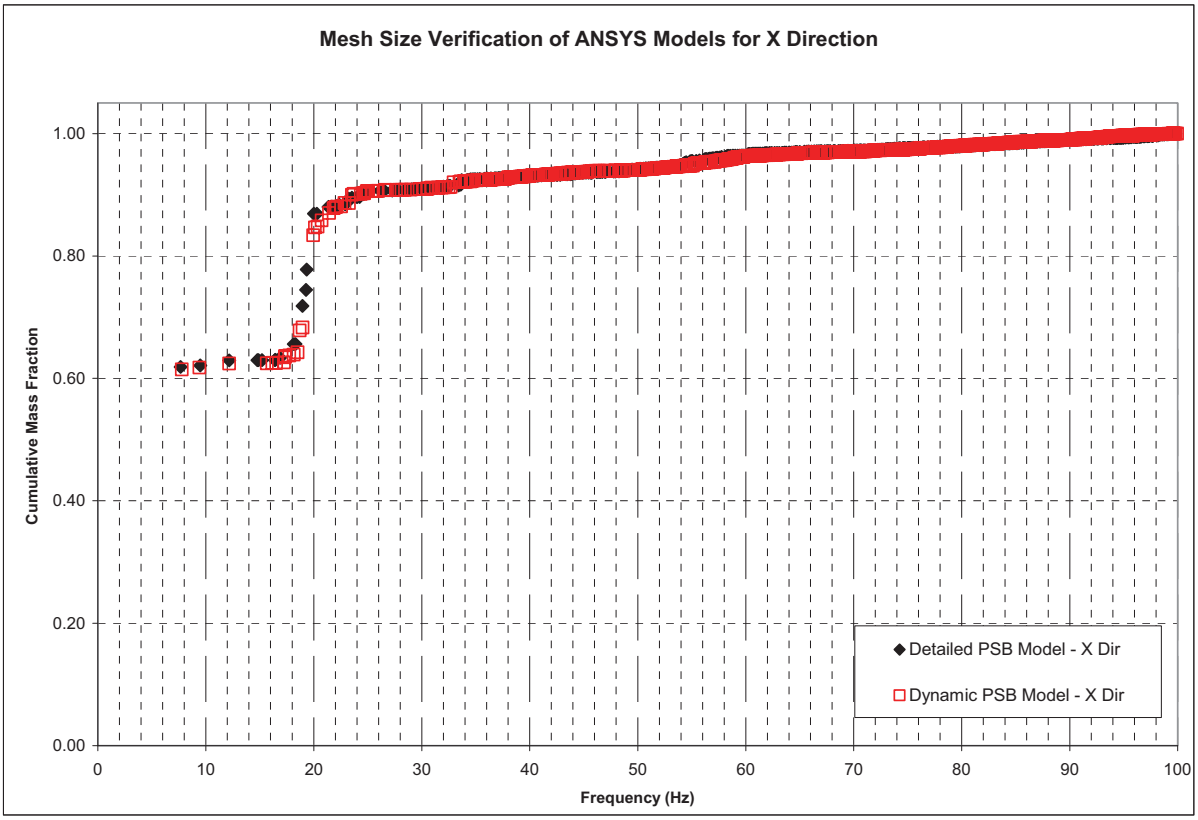

Figure 5.4.3-9 PS/B Modal Analysis Results – Cumulative Mass in the NS Direction (X)

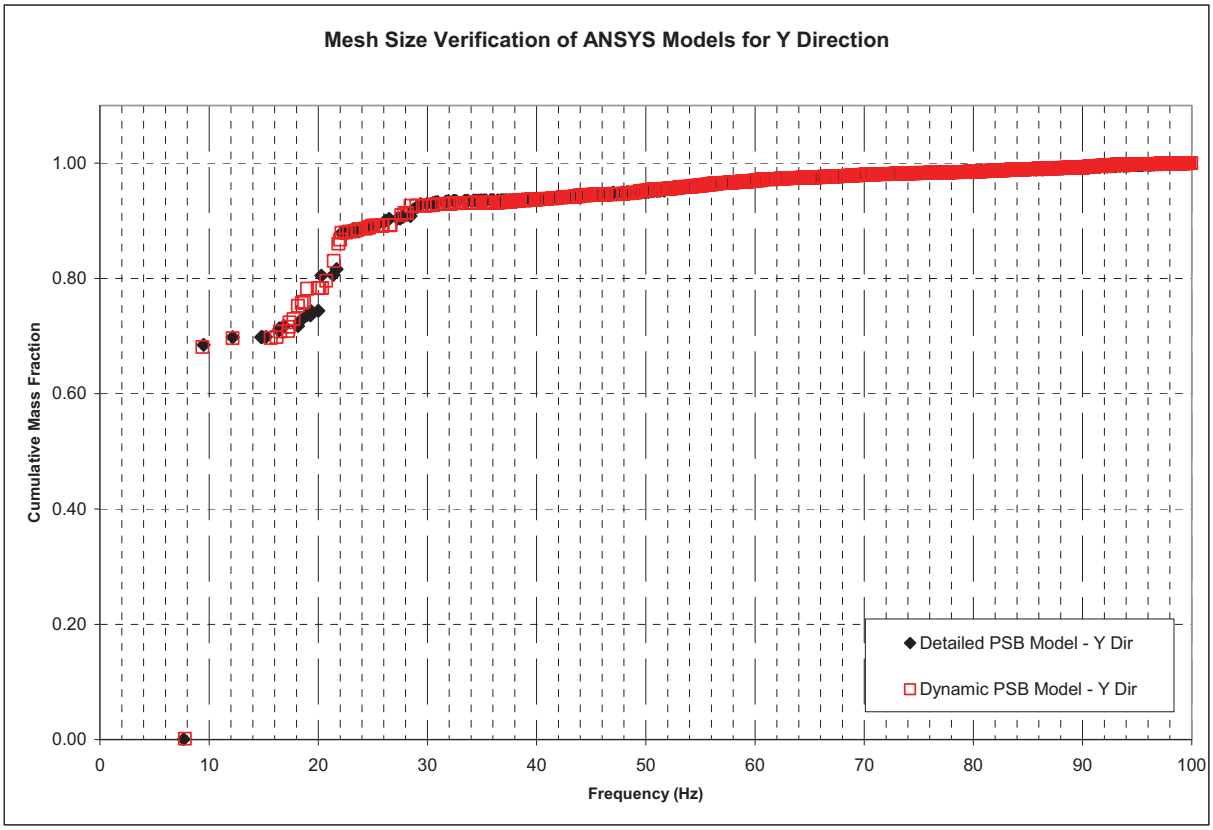

Figure 5.4.3-10 PS/B Modal Analysis Results – Cumulative Mass in the EW Direction (Y)

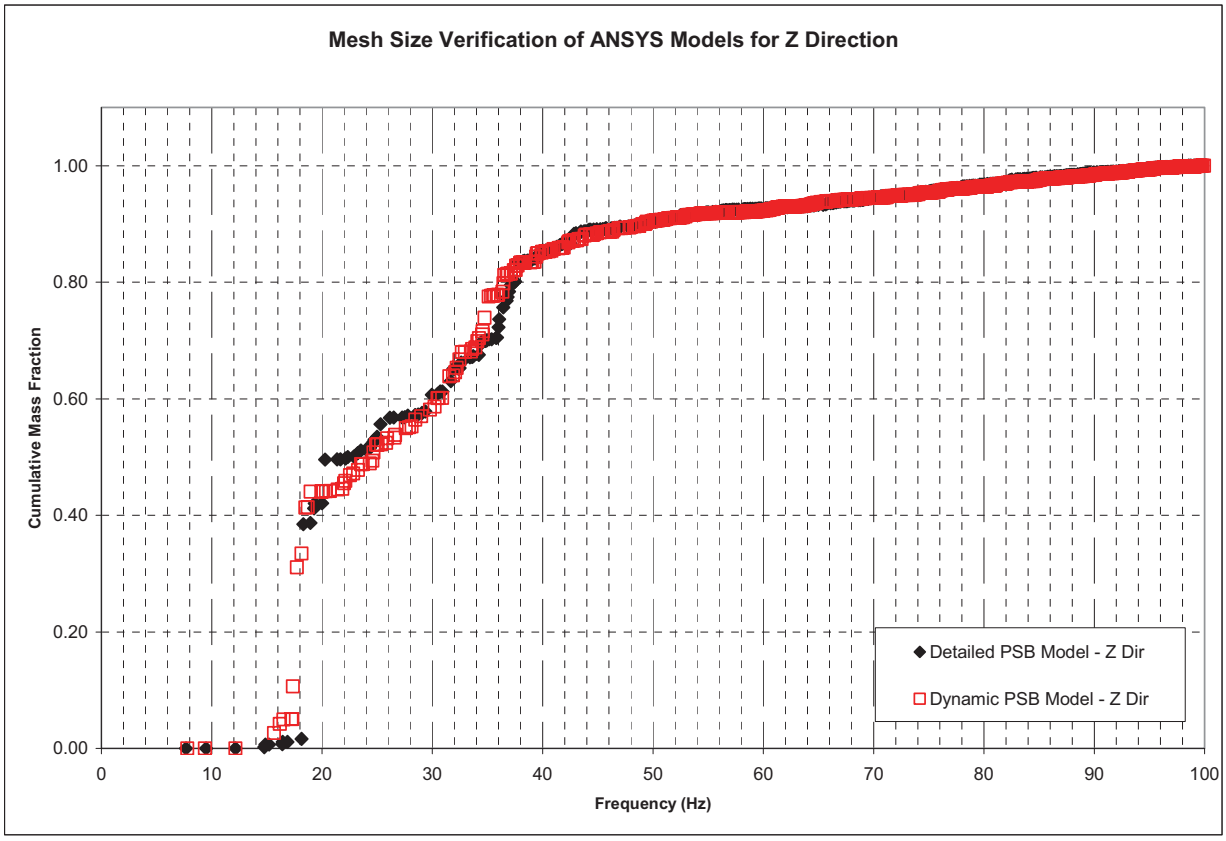

Figure 5.4.3-11 PS/B Modal Analysis Results – Cumulative Mass in the Vertical Direction (Z)

5.4.7.3 Modal Superposition Time History Analysis

A dynamic time-history response analysis using modal superposition is performed on both PS/B models using ANSYS. Acceleration response spectra (ARS) with 5% damping are generated for each model at various locations. These acceleration response spectra indicate that the Dynamic FE Model captures the structure response to dynamic loads in all directions properly. Figure 5.4.3-12 through Figure 5.4.3-20 show the comparison of Detailed and Dynamic FE Model ARS for representative locations. Generally, results of ARS from both modes are comparable and negligible deviations are observed. Figure 5.4.3-14 shows marginal difference between two models for the Z direction response due to Z direction excitations. The difference is contributed to the factors that the compared locations are not exactly same locations for the two models and the geometry (span) of the slabs in the two models are slightly different. The impact of this difference on the ISRS of the floor is expected to be minimal because the ISRS will be obtained from enveloping and broadening the SSI analysis results from the model with two level of stiffness.

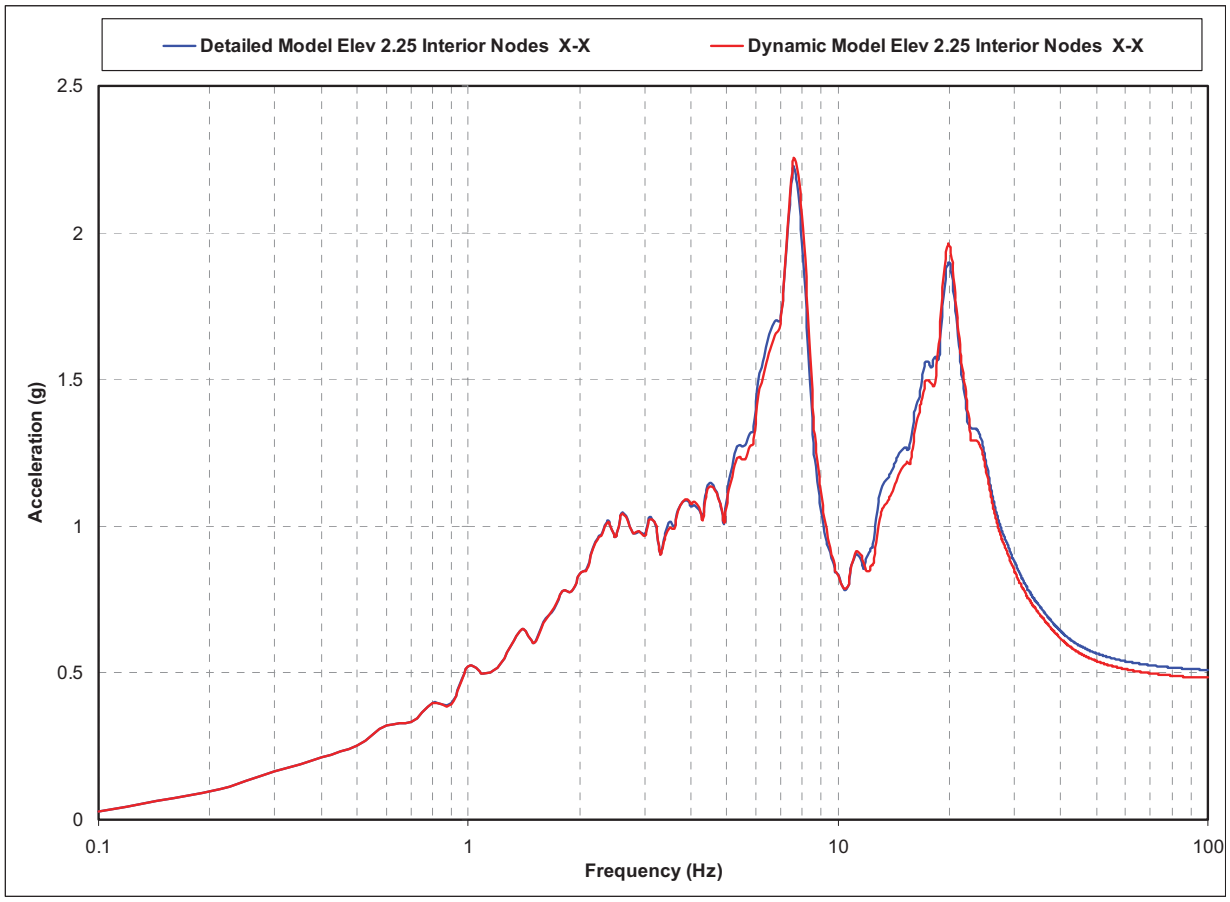

Figure 5.4.3-12 PS/B ARS Results – Comparison at Elev. 3'-7" Interior, X-direction

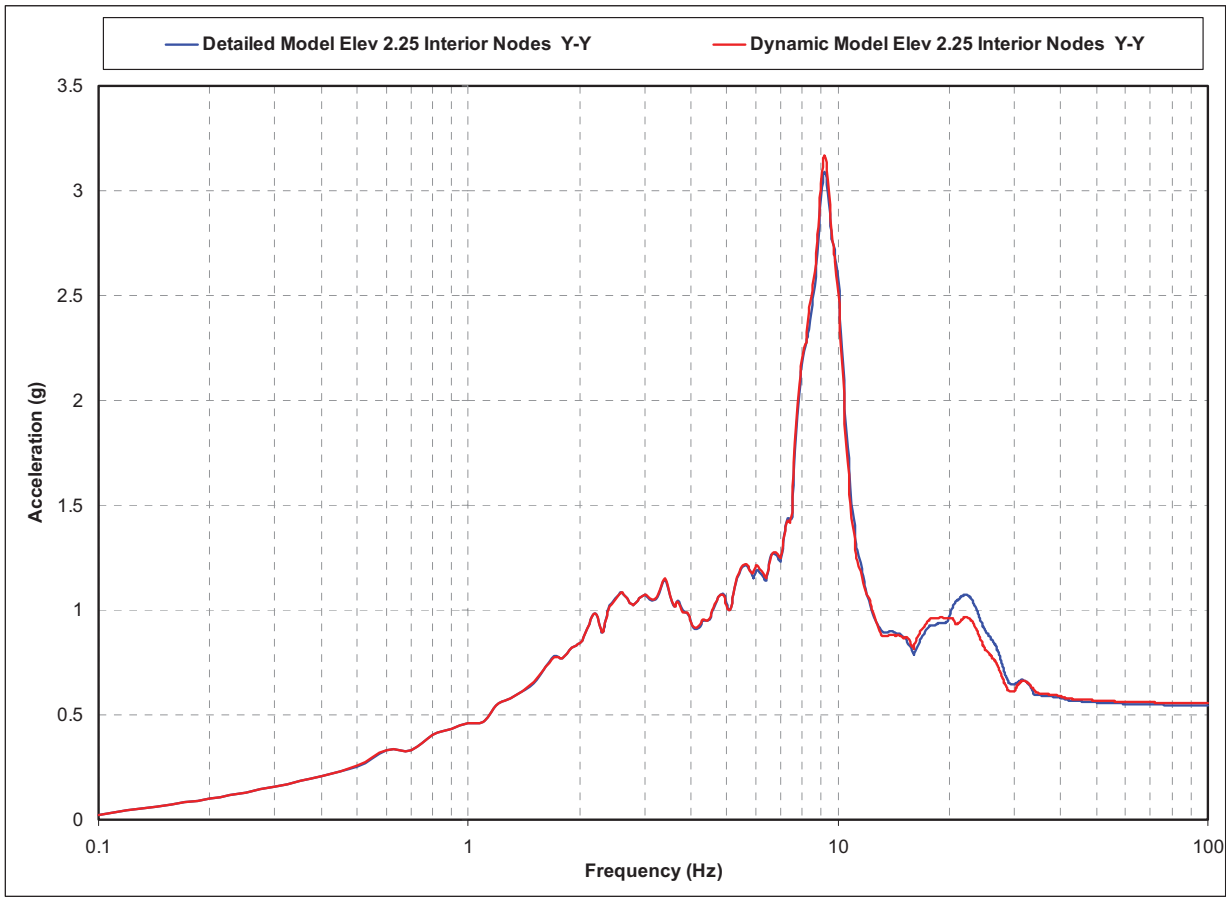

Figure 5.4.3-13 PS/B ARS Results – Comparison at Elev. 3'-7" Interior, Y-direction

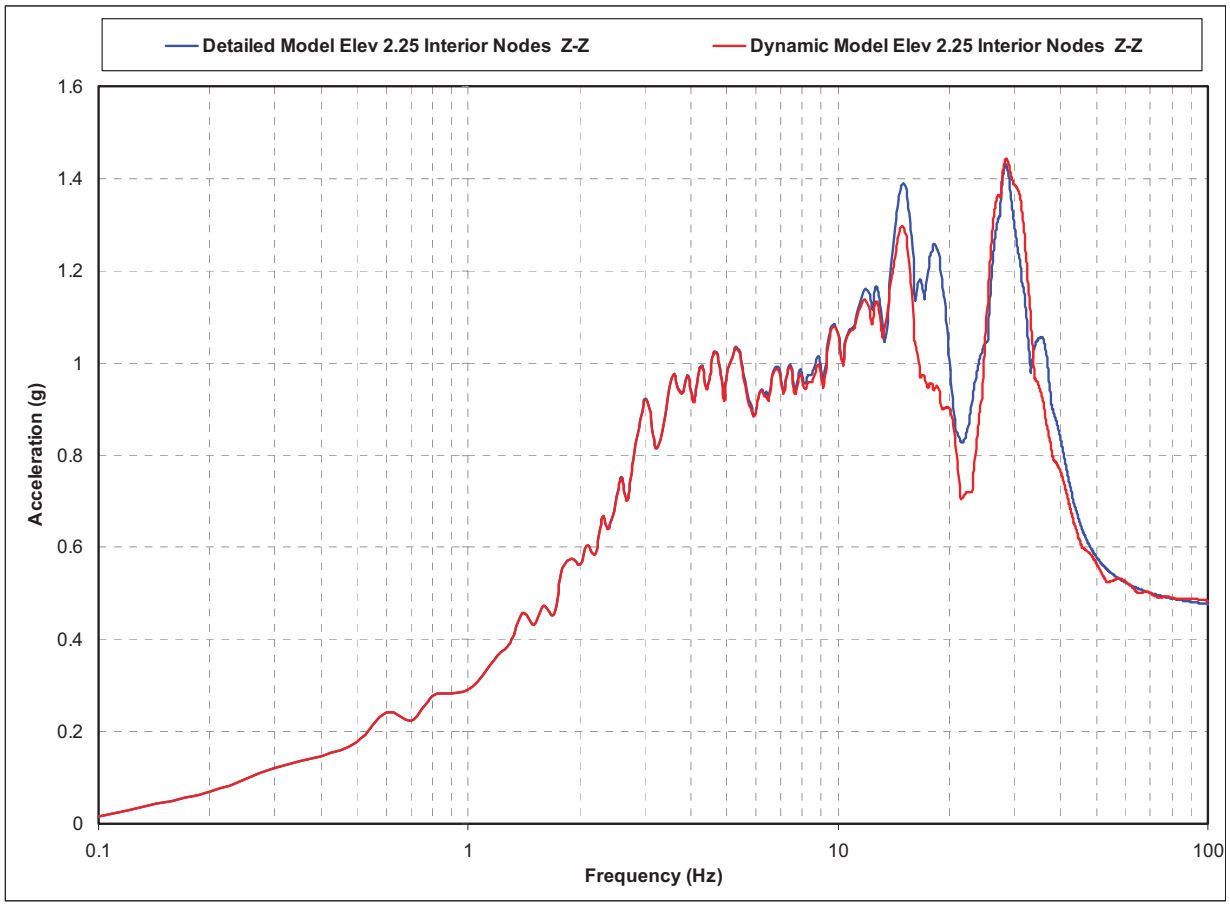

Figure 5.4.3-14 PS/B ARS Results – Comparison at Elev. 3'-7" Interior, Z-direction

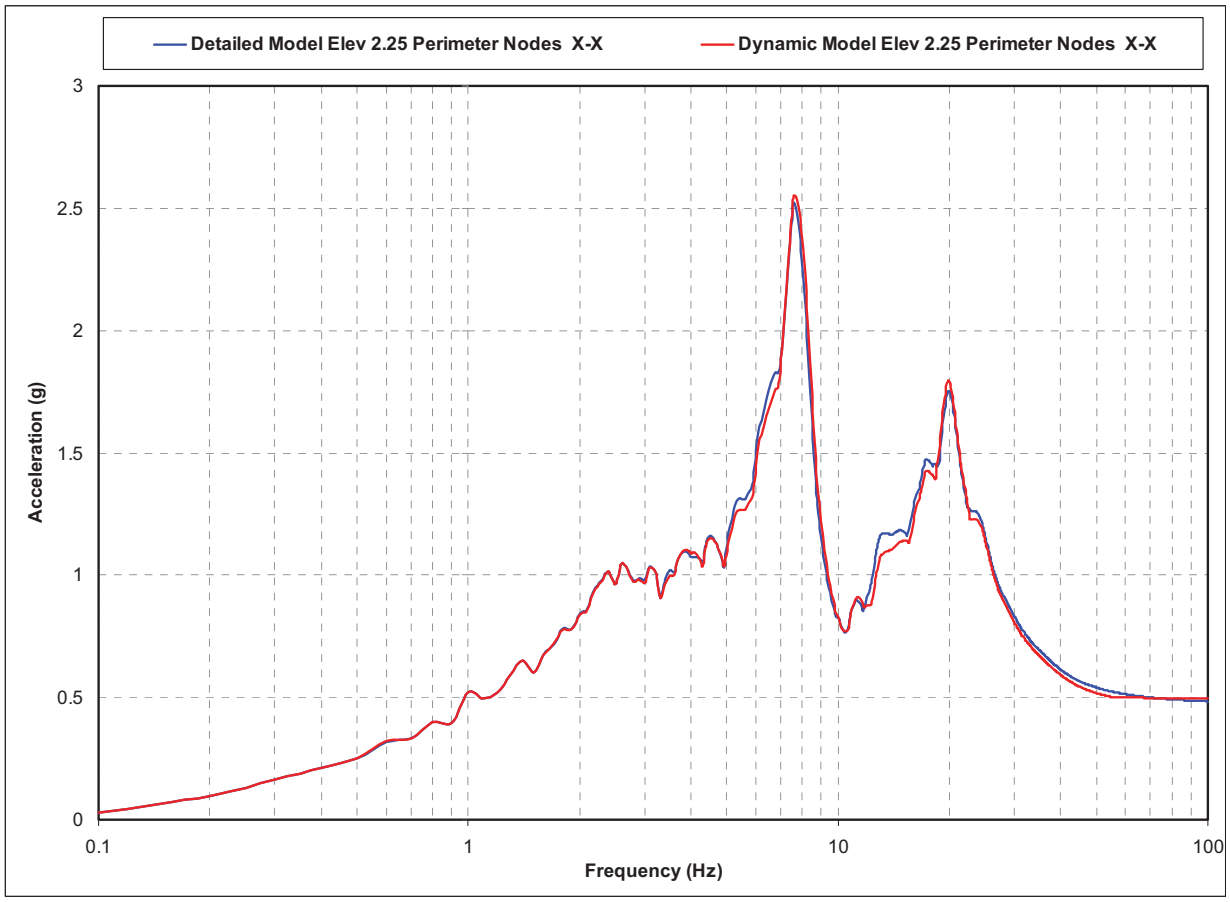

Figure 5.4.3-15 PS/B ARS Results – Comparison at Elev. 3'-7" Perimeter, X-direction

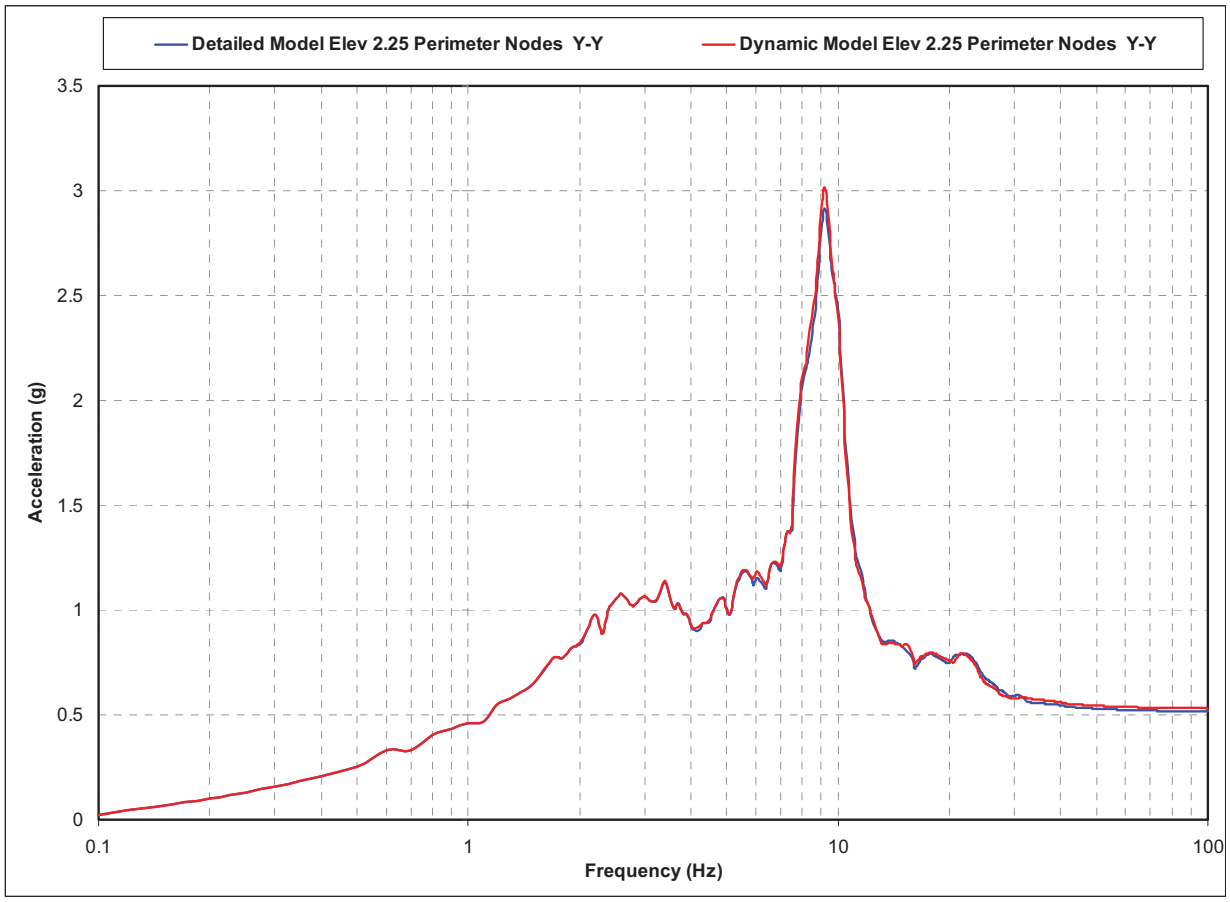

Figure 5.4.3-16 PS/B ARS Results – Comparison at Elev. 3'-7" Perimeter, Y-direction

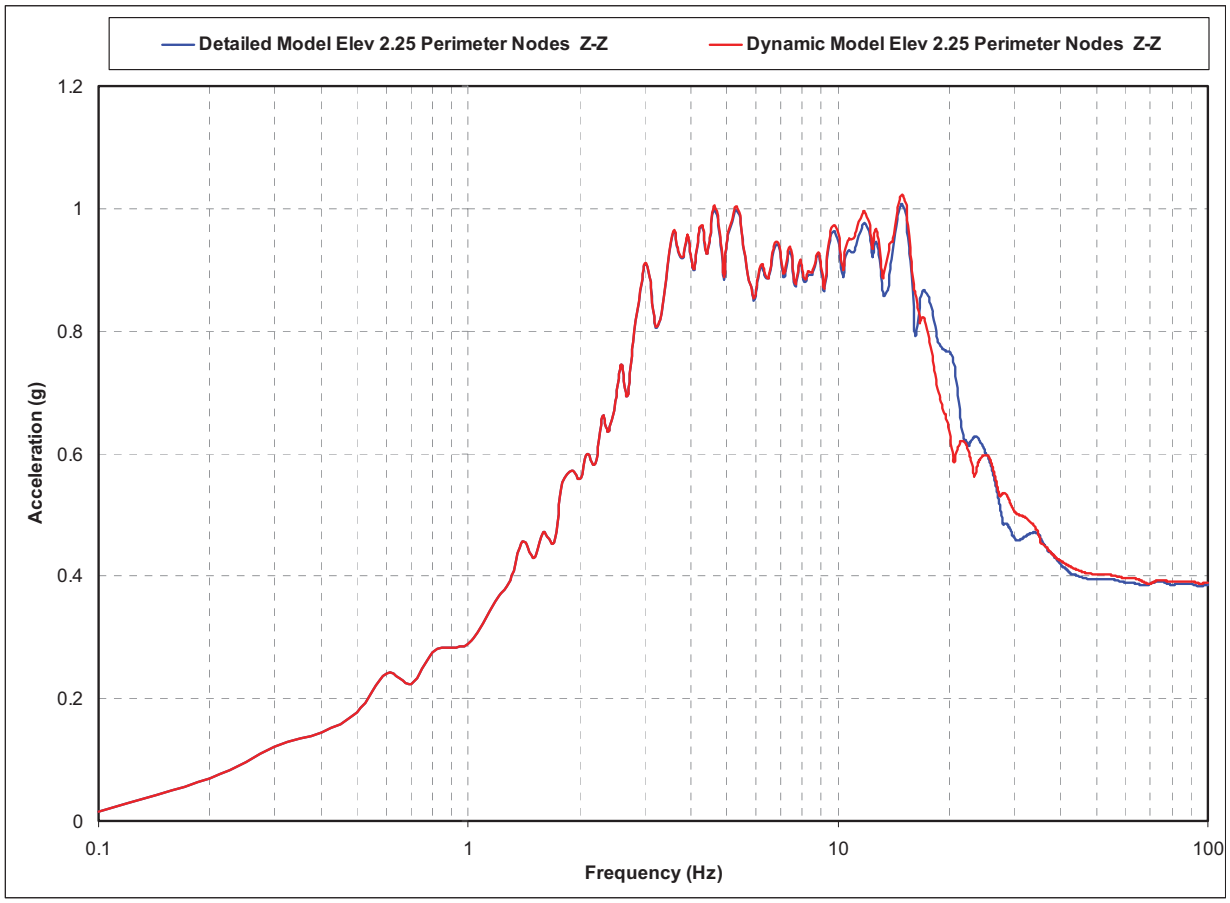

Figure 5.4.3-17 PS/B ARS Results – Comparison at Elev. 3'-7" Perimeter, Z-direction

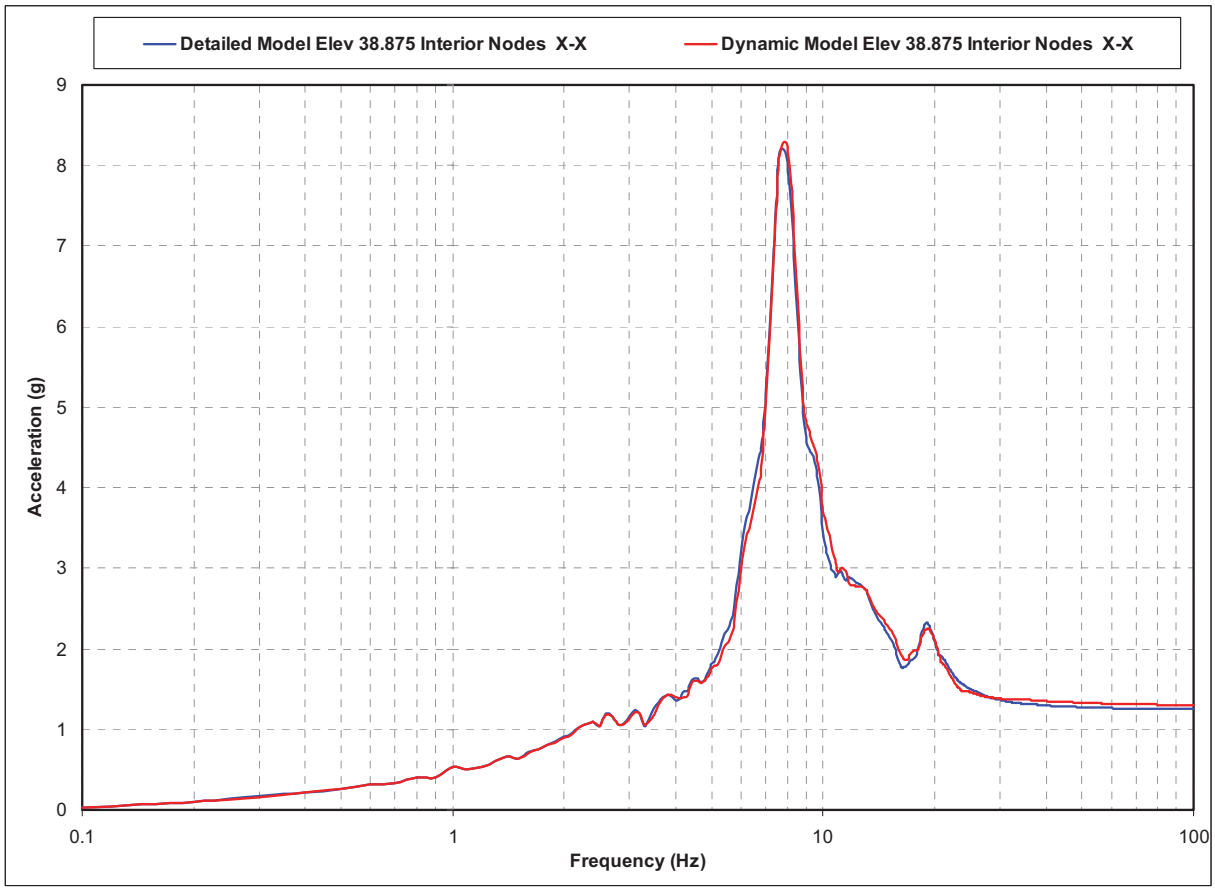

Figure 5.4.3-18 PS/B ARS Results – Comparison at Elev. 39'-6" Interior, X-direction

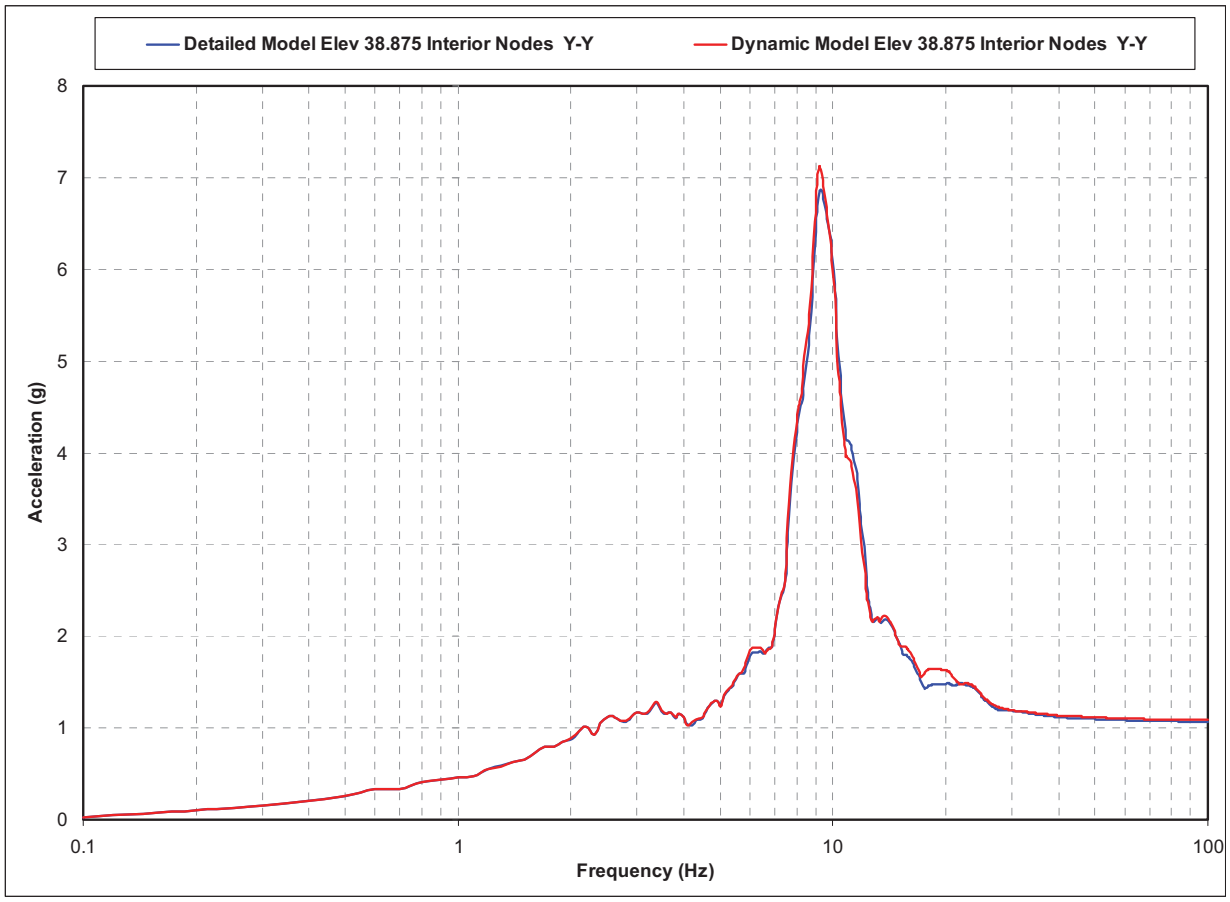

Figure 5.4.3-19 PS/B ARS Results – Comparison at Elev. 39'-6" Interior, Y-direction

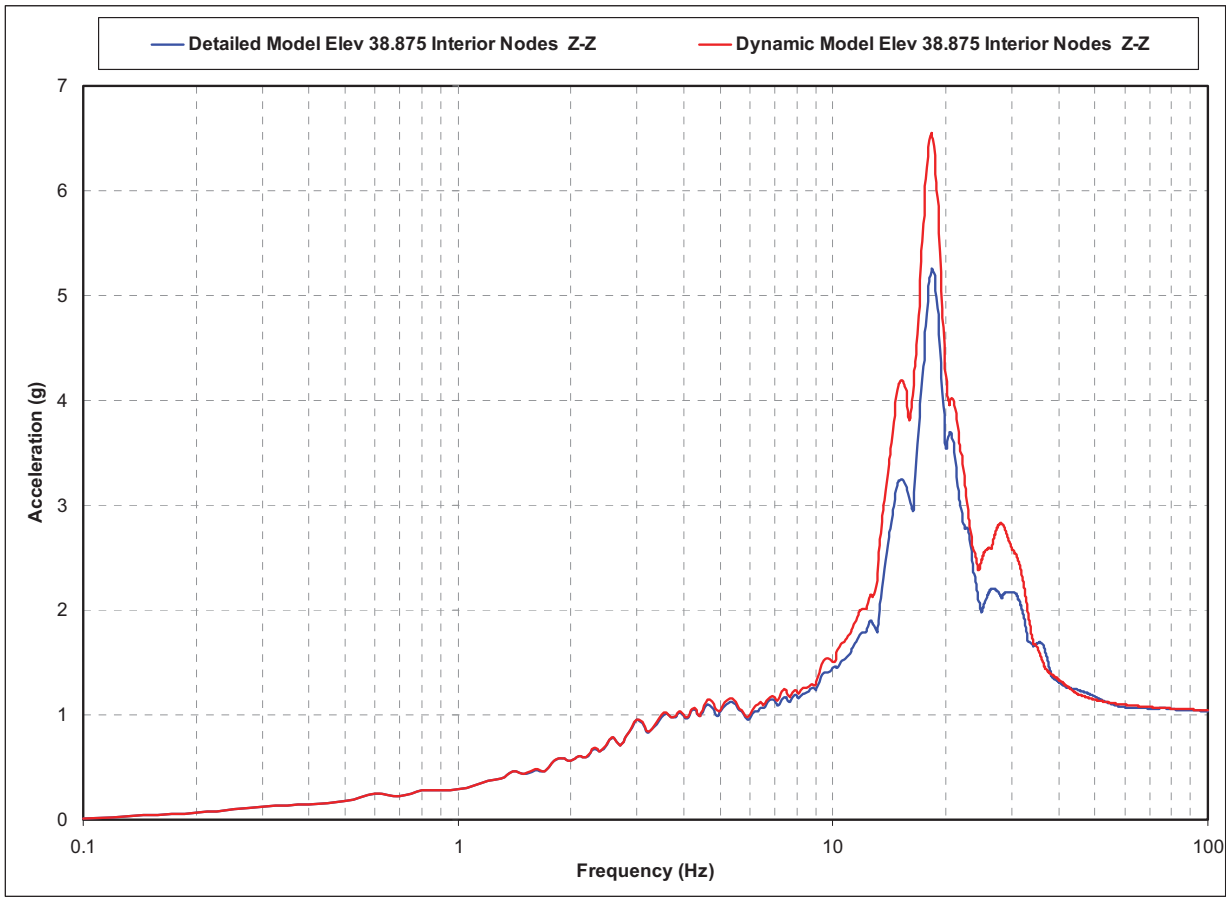

Figure 5.4.3-20 PS/B ARS Results – Comparison at Elev. 39'-6" Interior, Z-direction

5.4.8 Local Out-of-Plane Vibration of the Slabs

As discussed in Section 4.4.2, the dynamic properties, i.e., mass and stiffness (modulus of elasticity), of the flexible slabs with frequency below 70 Hz are checked by performing a series of modal analyses using ANSYS on isolated sub-models at each elevation. The first 3 dominant frequencies of each slab from the original models are obtained and the frequencies compared. The frequencies of all major slabs were found to match those of the Detailed FE model. The results from these analyses are presented hereafter.

Figure 5.4.4-1 to Figure 5.4.4-4 are a sample of the plots obtained from the modal analysis performed on the isolated elevations of the Detailed and Dynamic FE model using ANSYS.

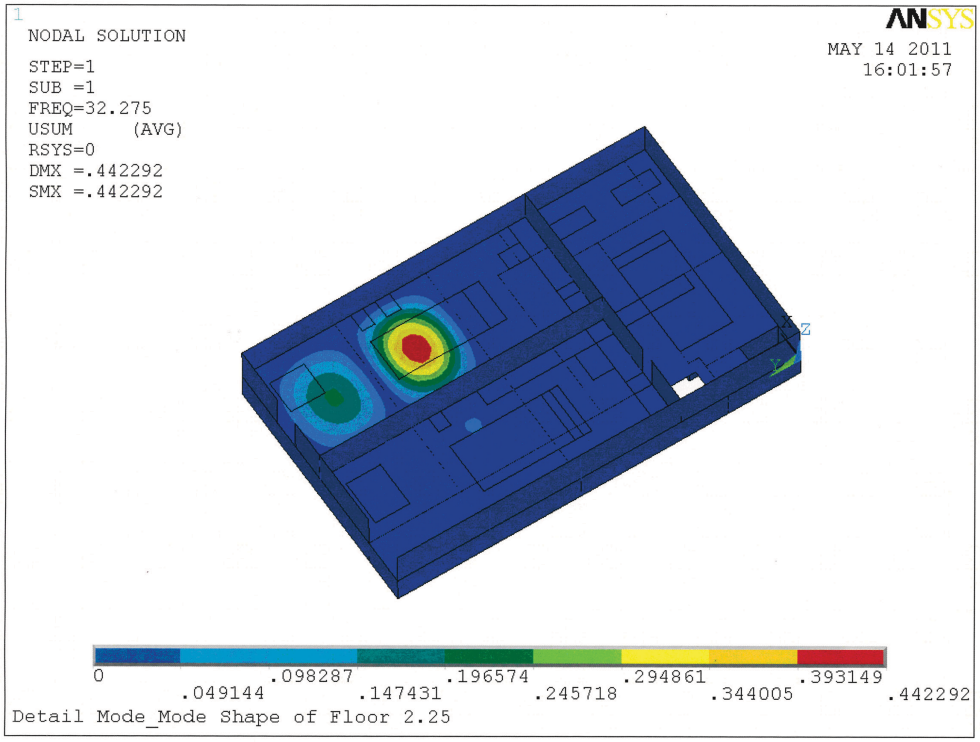

Figure 5.4.4-1 Ground Floor (EL. 3'-7") – Detailed Model - 1st Dominant Frequency

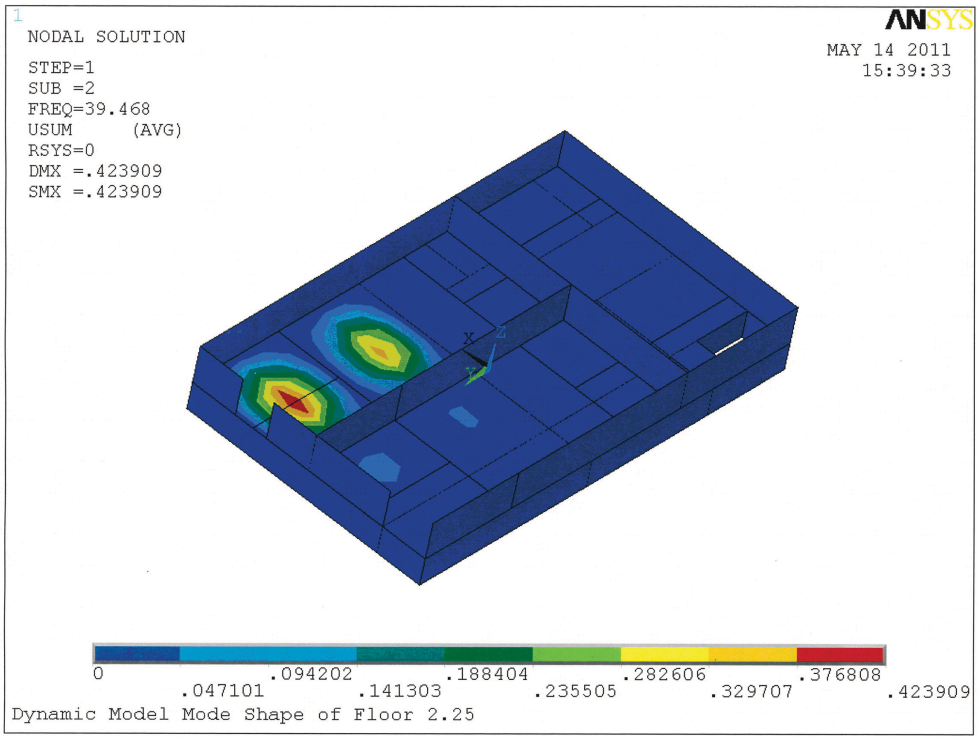

Figure 5.4.4-2 Ground Floor (EL. 3'-7") – Dynamic Model - 1st Dominant Frequency

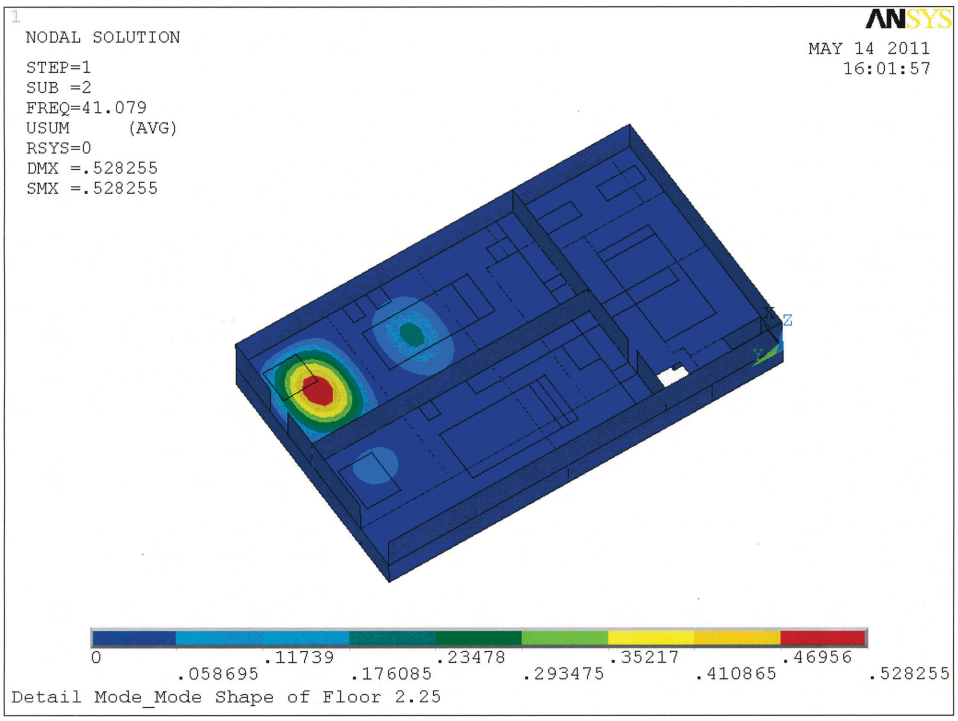

Figure 5.4.4-3 Ground Floor (EL. 3'-7") – Detailed Model – 2nd Dominant Frequency

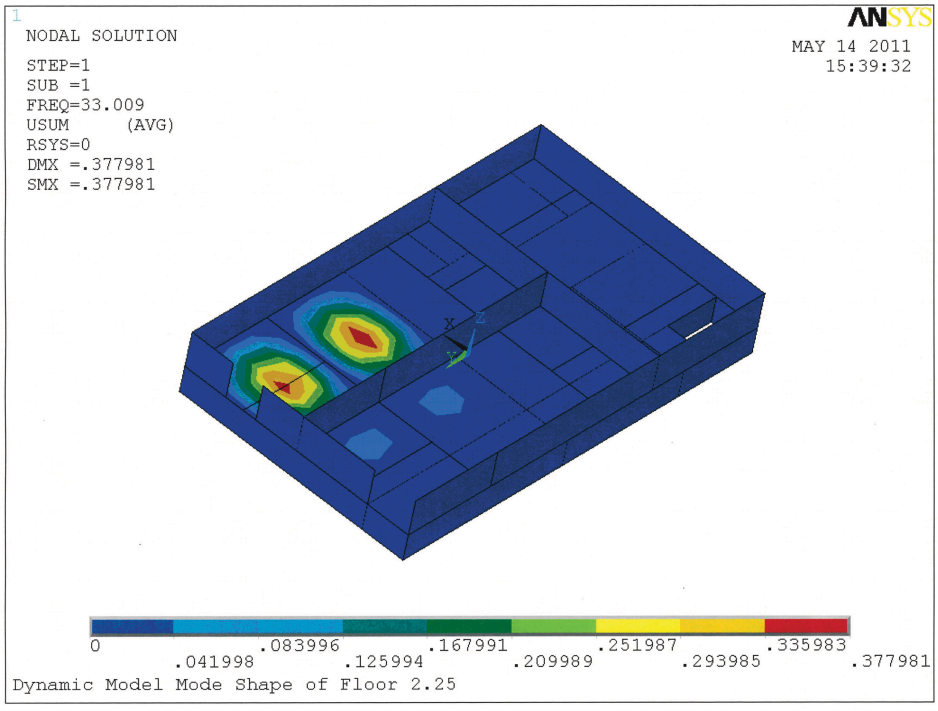

Figure 5.4.4-4 Ground Floor (EL. 3'-7") – Dynamic Model – 2nd Dominant Frequency

5.4.9 ACS SASSI Validation

After the Dynamic FE Model is validated against the Detailed FE Model, it is translated into ACS SASSI (Reference 2) using the built in file converter. To confirm that the translation is accurate and correct, an analysis is run with the PS/B model sitting on hard rock to simulate a fixed base condition. Transfer functions from this analysis are compared with the modal analysis results of the Dynamic FE Model to ensure that the mass and stiffness properties are accurate. Response spectra produced are also compared with the ARS from the Dynamic FE Model to ensure that the structural response is accurate as well. Figures 5.4.5-1 through 5.4.5-3 show the transfer function plots. These plots indicate that the ACS SASSI model accurately captures the dynamic properties of the PS/B when compared against the validated Dynamic FE Model. Figures 5.4.5-4 through 5.4.5-9 present the ACS SASSI response spectra compared to the Dynamic FE Model ARS for selected group of nodes. The ARS curves in the plots are the envelope of ARS of the corresponding group of nodes. In the plots, label with “ACS SASSI” indicates the curves are the results of SSI analysis performed on the model sitting on rigid half space while label with “Dynamic Model” indicates the curves are obtained from ANSYS modal superposition time history analysis performed on the model with fixed base boundary condition. The comparison shows that the ACS SASSI model accurately represents the structural response of the validated Dynamic FE Model. Differences are observed from the figures for the analysis results using two different codes. They are acceptable based on acceptance criteria and justifications discussed in Section 4.3.3 of this report.

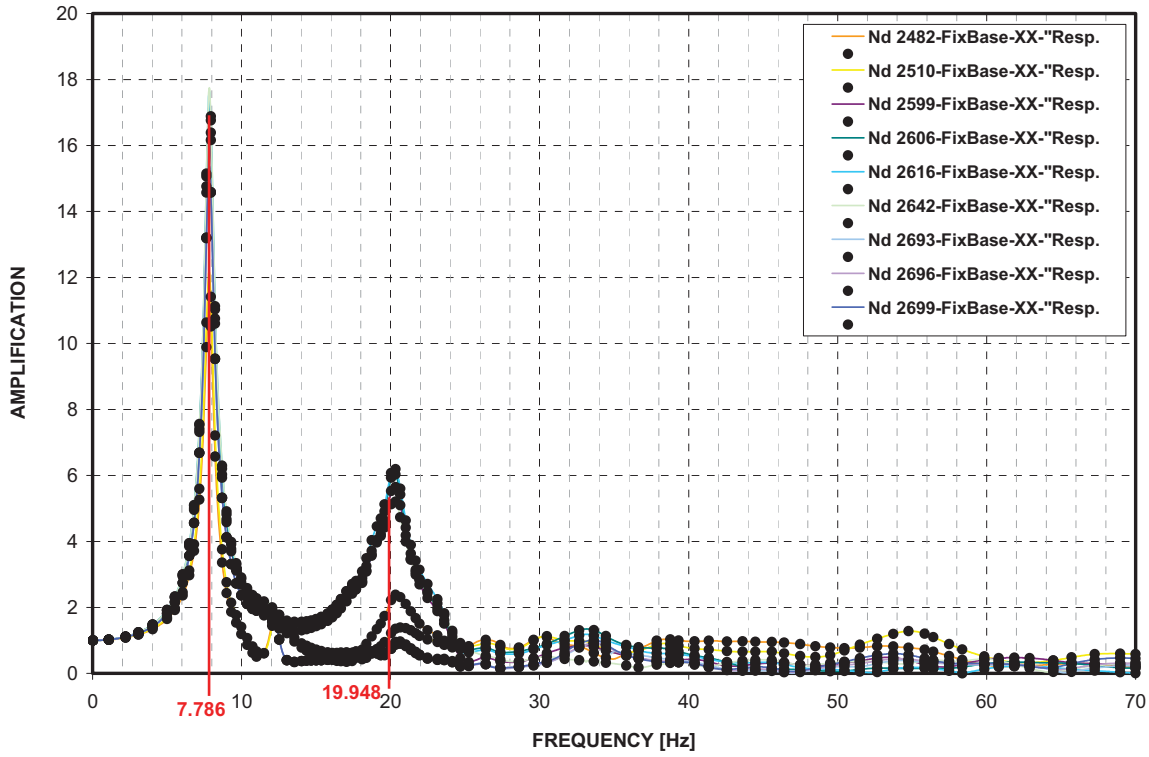

Figure 5.4.5-1 PS/B ACS SASSI Results – Transfer Functions NS Direction

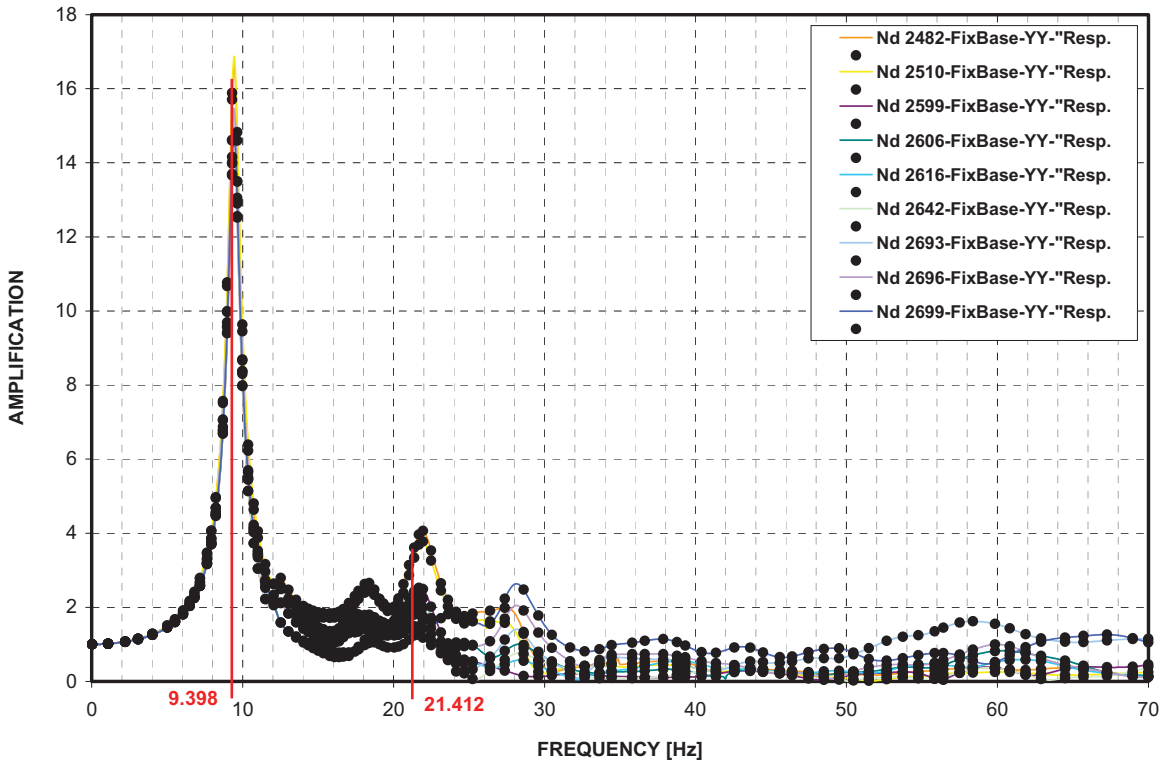

Figure 5.4.5-2 PS/B ACS SASSI Results – Transfer Functions EW Direction

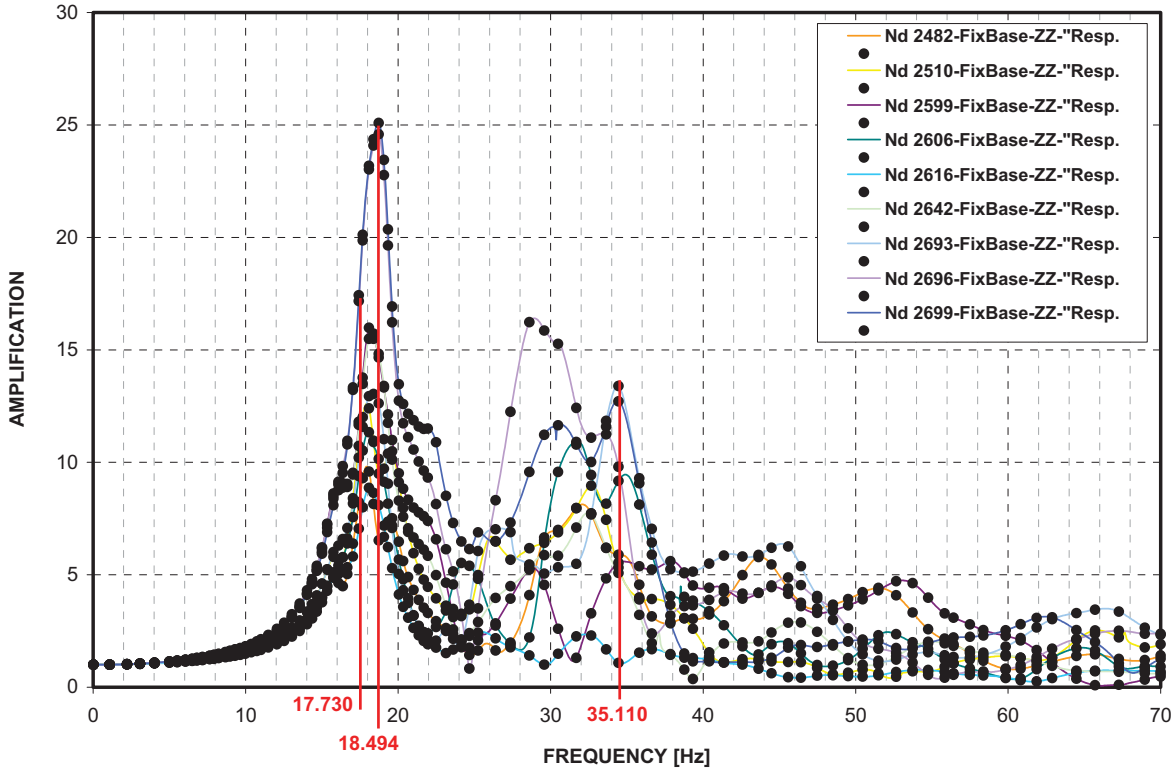

Figure 5.4.5-3 PS/B ACS SASSI Results – Transfer Functions Vertical Direction

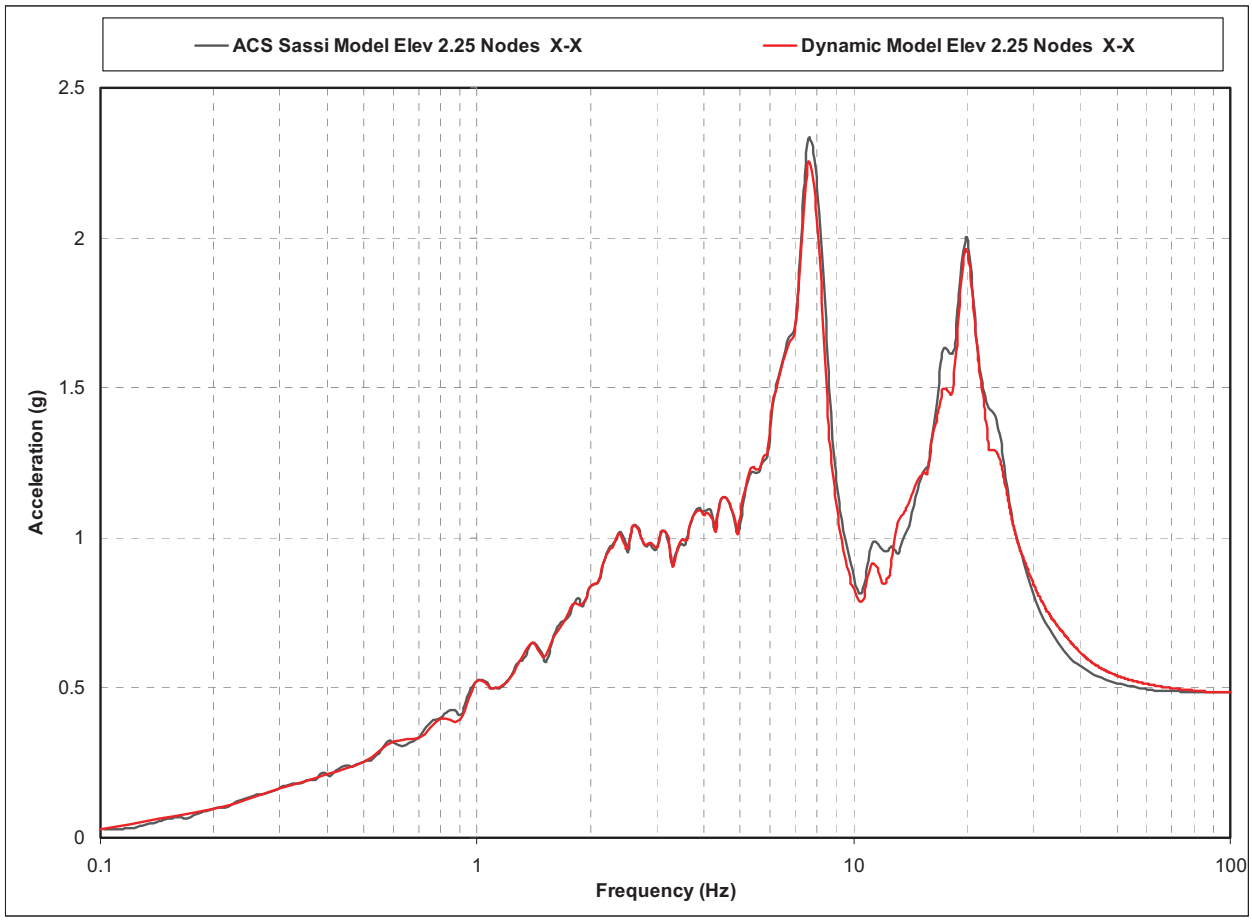

Figure 5.4.5-4 PS/B ACS SASSI Results – ARS Comparison at Elev. 3'-7" X-direction

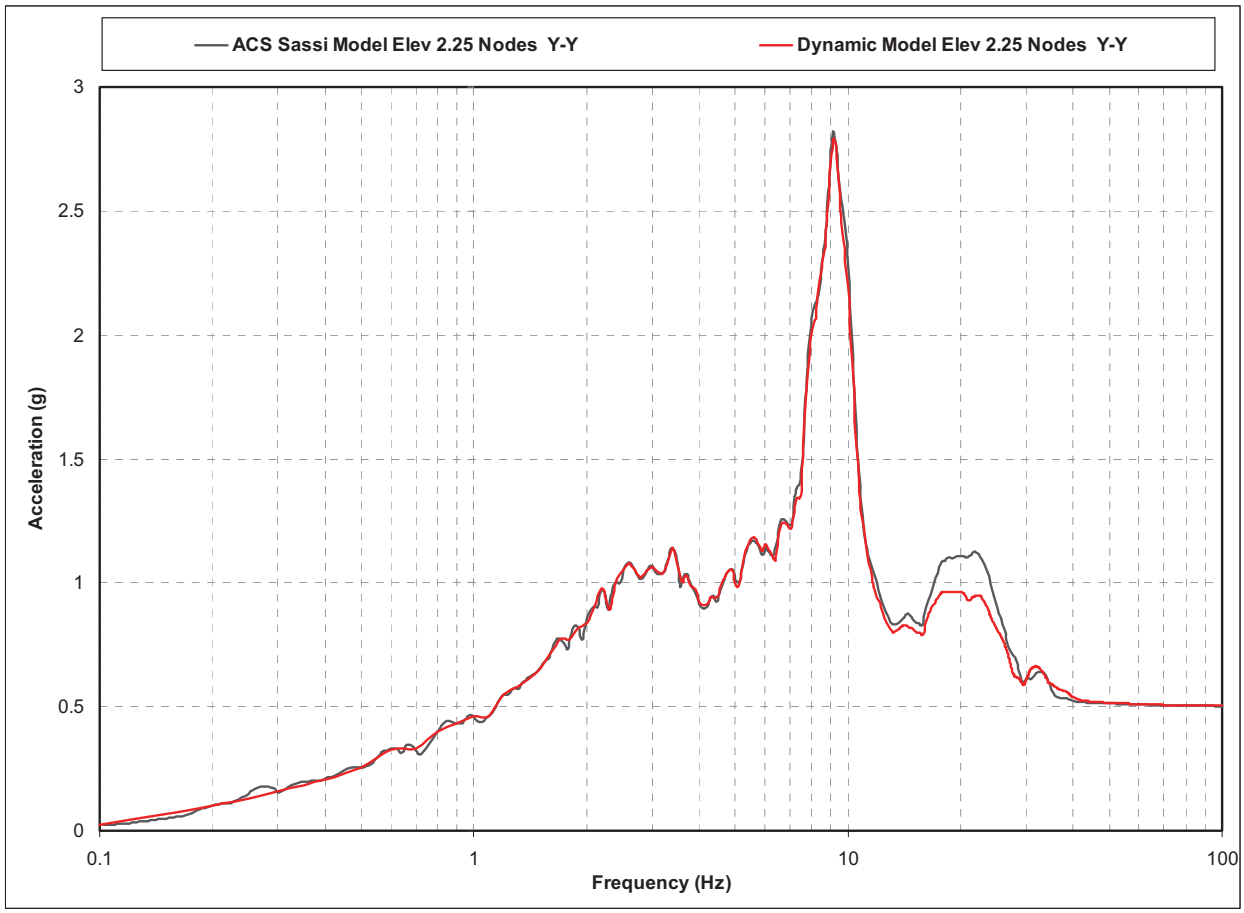

Figure 5.4.5-5 PS/B ACS SASSI Results – ARS Comparison at Elev. 3'-7" Y-direction

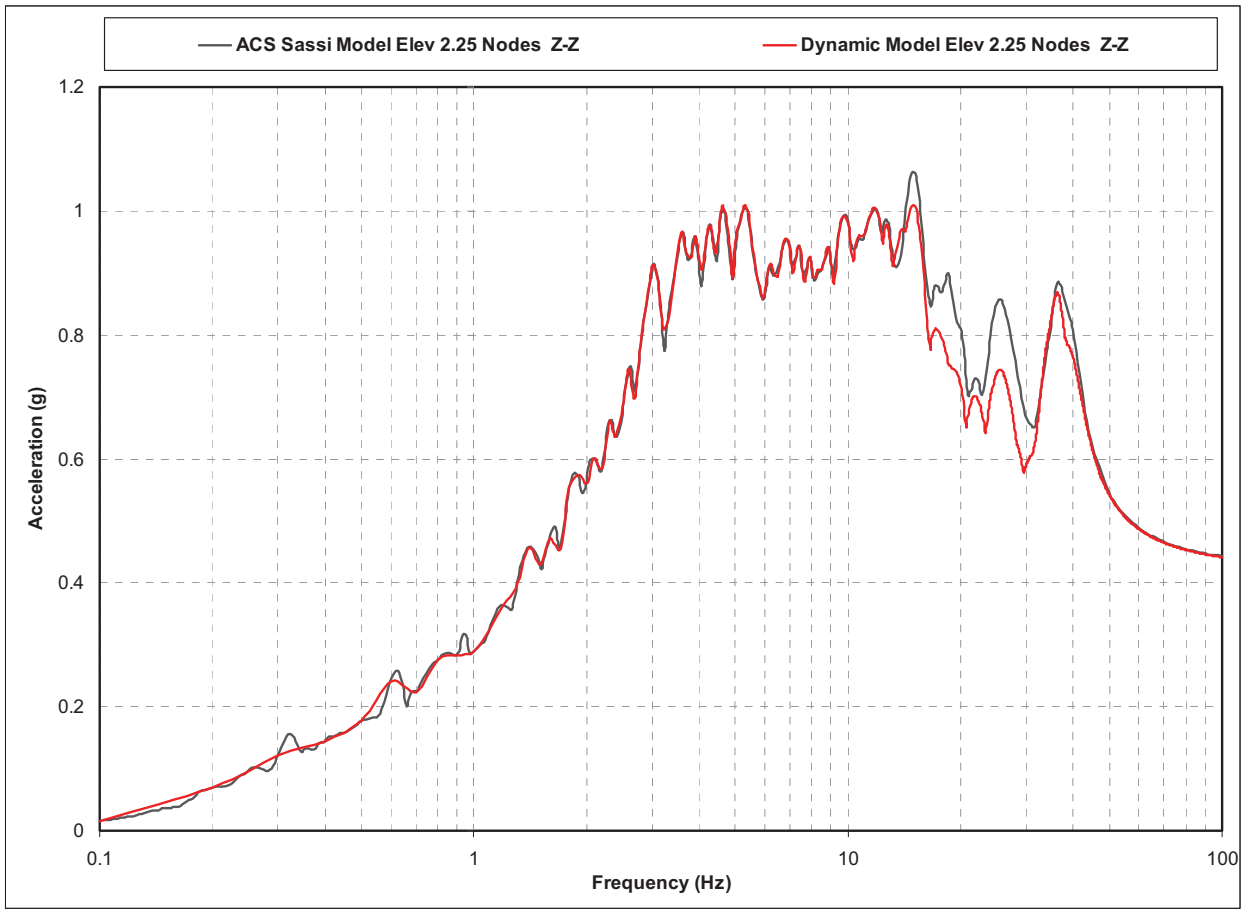

Figure 5.4.5-6 PS/B ACS SASSI Results – ARS Comparison at Elev. 3'-7" Z-direction

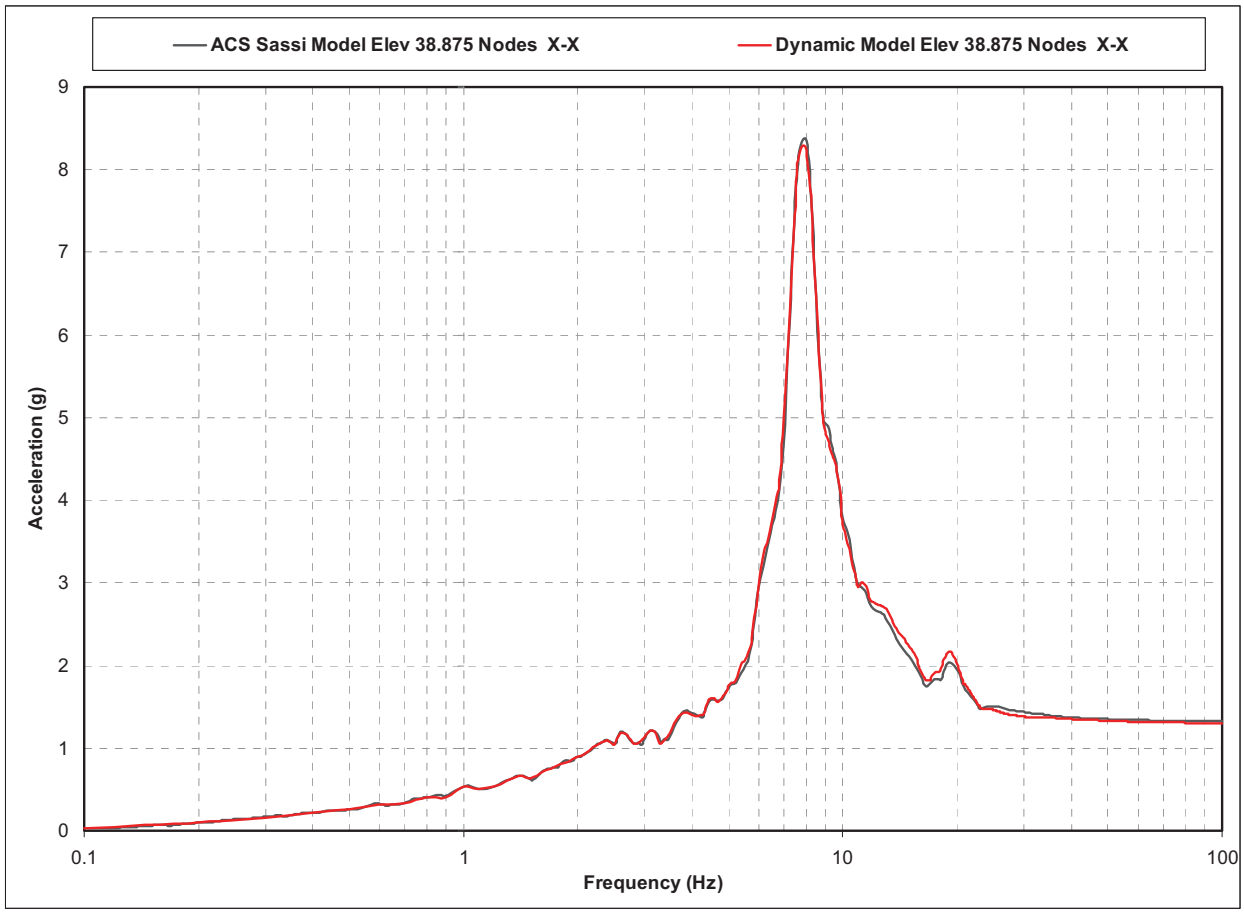

Figure 5.4.5-7 PS/B ACS SASSI Results – ARS Comparison at Elev. 39'-6" X-direction

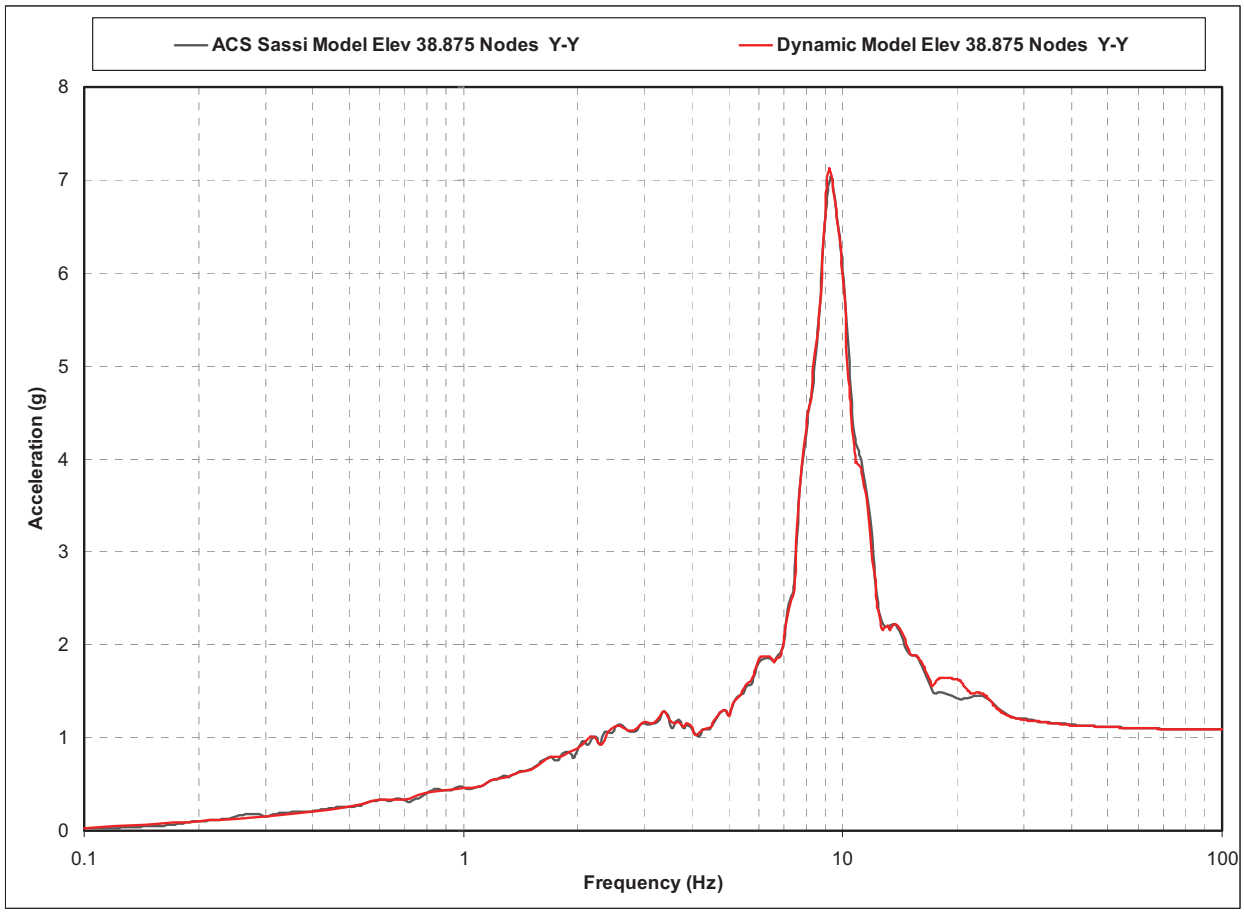

Figure 5.4.5-8 PS/B ACS SASSI Results – ARS Comparison at Elev. 39'-6" Y-direction

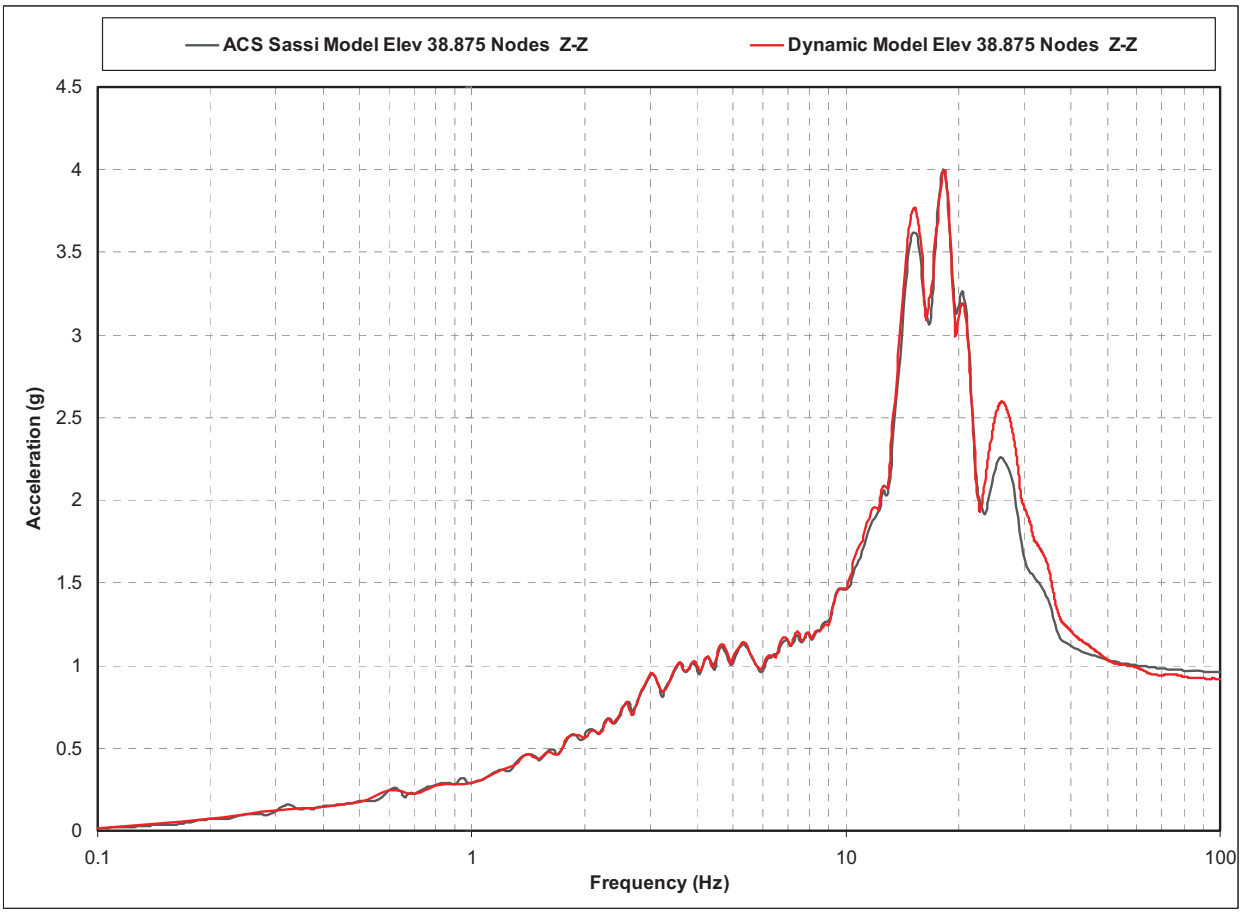

Figure 5.4.5-9 PS/B ACS SASSI Results – ARS Comparison at Elev. 39'-6" Z-direction

5.4.10 Results and Conclusion

Figures 5.4.6-1, 5.4.6-2 and 5.4.6-3 present the Dynamic FE model developed for the SSI analysis of the US-APWR East and West Power Source Buildings. Developed using ANSYS preprocessor before being translated into ACS SASSI, this model is generated only for the West PS/B but it represents both buildings since both are nearly identical structurally. The overall dimensions of the model are 69'-4" in the N-S direction by 114'-10" in the E-W direction, resulting in a total footprint area of 7,962 ft^2. The model weighs 41,845 kips in total, with an average contact pressure under the foundation of about 5.3 ksf.

Based on the results of the validation analyses summarized in this report, it can be concluded that the Dynamic FE model of the PS/B truly represents the dynamic properties of the two PS/B structures. Table 5.4.6-1 presents the dominant frequencies of the PS/B Dynamic FE model with full stiffness, while Figures 5.4.6-1 to 5.4.6-2 show additional section views of the model. A structure overview and other sectional views of the model are presented in figures 5.4.1-1 through 5.4.1-7.

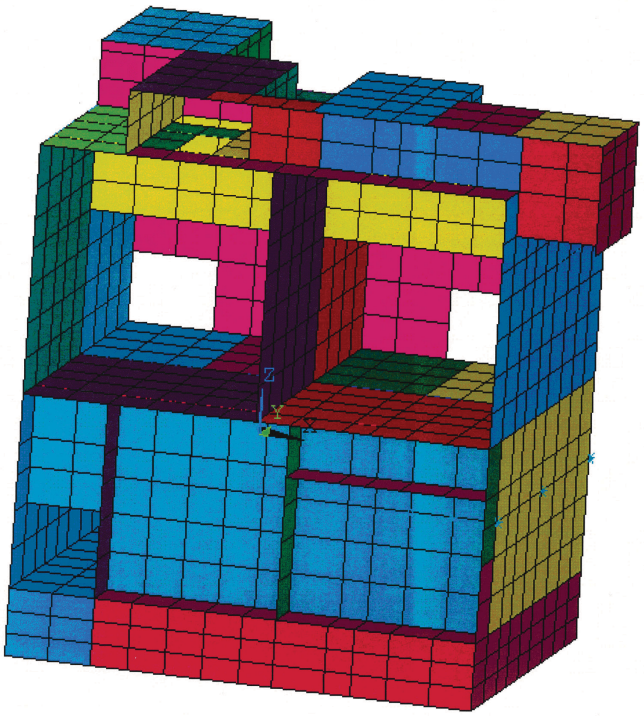

Figure 5.4.6-1 Section View of Dynamic PS/B Model Looking East

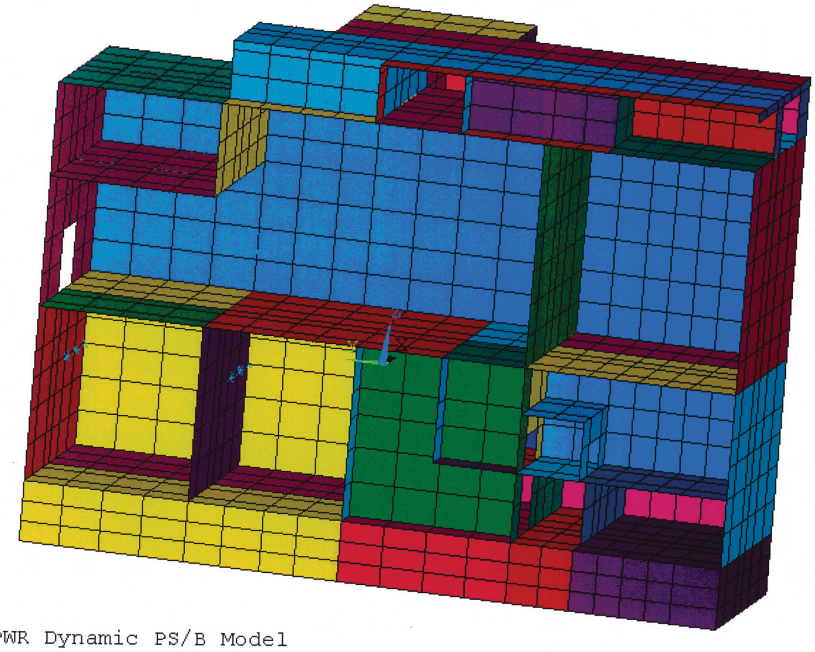

Figure 5.4.6-2 Section View of Dynamic PS/B Model Looking South

Table 5.4.6-1 Dominant Frequencies of the PS/B Dynamic FE Model

NS Direction (X)		EW Direction (Y)		Vertical Direction (Z)	
Mode	Frequency (Hz)	Mode	Frequency (Hz)	Mode	Frequency (Hz)
1	7.8	2	9.4	9	17.4
13	18.7	11	18.1	10	17.7
15	19.9	19	21.4	12	18.5
26	23.5	20	21.9	48	31.5